Label-free Nanoplasmonic Sensing of Tumor-Associate Autoantibodies for Early Diagnosis of Colorectal Cancer

Maria Soler[a,b,†], M.-Carmen Estevez[b,a,*], Roi Villar-Vazquez[c], J. Ignacio Casal[c] and Laura M. Lechuga[a,b]

[a]Nanobiosensors and Bioanalytical Applications Group (NanoB2A), Catalan Institute of Nanoscience and Nanotechnology (ICN2), CSIC and The Barcelona Institute of Science and Technology, Campus UAB, Bellaterra, 08193 Barcelona, Spain

[b]CIBER-BBN Networking Center on Bioengineering, Biomaterials and Nanomedicine, Spain

[c]Functional Proteomics Group, Centro de Investigaciones Biológicas (CIB-CSIC), 28040 Madrid, Spain

[†]*Present address*: Bionanophotonic Systems Laboratory (BIOS, STI-IBI), Ecole Polytechnique Federale de Lausanne (EPFL), CH 1015 Lausanne, Switzerland

**Corresponding Author*:

M.-Carmen Estevez

NanoBiosensors and Bioanalytical Applications Group
Catalan Institute of Nanoscience and Nanotechnology (ICN2), CSIC and The Barcelona Institute of Science and Technology and CIBER-BBN
Campus de la UAB, Edifici ICN2
08193 Bellaterra (Barcelona) Spain

Tel:+34937374629

email:mcarmen.estevez@cin2.es

ABSTRACT

Colorectal cancer is treatable and curable when detected at early stages. However there is a lack of less invasive and more specific screening and diagnosis methods which would facilitate its prompt identification. Blood circulating autoantibodies which are immediately produced by the immune system at tumor appearance have become valuable biomarkers for preclinical diagnosis of cancer. In this work, we present the rapid and label-free detection of colorectal cancer autoantibodies directly in blood serum or plasma using a recently developed nanoplasmonic biosensor. Our nanoplasmonic device offers sensitive and real-time quantification of autoantibodies with excellent selectivity and reproducibility, achieving limits of detection around 1 nM (150-160 $ng \cdot mL^{-1}$). A preliminary evaluation of clinical samples of colorectal cancer patients has shown good correlation with ELISA. These results demonstrate the reliability of the nanobiosensor strategy and pave the way towards the achievement of a sensitive diagnostic tool for early detection of colorectal cancer.

Keywords

nanoplasmonic biosensor; plasma; serum; colorectal cancer; autoantibodies; clinical diagnosis

Abbreviations

CRC colorectal cancer

ELISA enzyme-linked immunosorbent assay

LSPR localized surface plasmon resonance

POC point of care

RI refractive index

SAM self-assembled monolayer

TAA tumor-associate antigen

1. Introduction

Colorectal cancer (CRC) is a worldwide health problem with an incidence over 1 million annual cases and being a major cause of morbidity and mortality in developed countries [1]. It is the third most common cancer and the fourth most common cause of death around the world. Despite the exact cause for CRC is not known, several risk factors have been established for the disease, including genetic and epigenetic parameters [2]. Familiar history of colon cancer or inflammatory diseases, age, lifestyle and environmental conditions are strongly associated to CRC development. CRC is easily curable when detected early [2], thereby prevention and regular screening play crucial roles in the fight against this cancer. However, CRC diagnosis is particularly challenging. The most reliable diagnosis technique is *via* sampling of colon biopsies suspected of possible tumor development, which is typically done during colonoscopy or sigmoidoscopy for the distal colon and rectum [3]. These procedures are highly invasive and present important limitations in terms of costs, available resources and low compliance. On the other hand, established noninvasive tests such as the guaiac-based fecal occult blood test (gFOBT) suffer from low specificity leading to inaccurate diagnosis results [4]. There is an evident need for novel screening tools, ideally, analytical techniques based on blood analysis, which permit the early and reliable identification and diagnosis of CRC. Development of blood biomarker assays that could indicate that a cancerous process is triggered would represent a great benefit. However, although a few serum proteins have been described as biomarkers in CRC (carcinoembryonic antigen (CEA), CA19.9 or CA125), none of them are recommended for early clinical diagnosis but for advanced stages and for monitoring recurrence of the disease [5].

Over the past decade, cancer research has made major advances in understanding the causes of developing CRC as well as the molecular mechanisms involved in the disease [6]. For instance many solid tumors such as breast, lung or colon cancer have revealed to be immunogenic. These tumors express aberrant levels of mutated or modified proteins known as tumor-associated antigens (TAA), which are related to the malignant growth. Such proteins can stimulate cellular and humoral immune response, triggering specific autoantibody production [7,8]. The role of autoantibodies in cancer is still unclear. It is not well-known whether they play a cancer-promoting role, an anti-tumor effect or if

they are an epiphenomenon associated to inflammation and tumor progression [9]. Nevertheless, autoantibody responses to TAAs hold promising characteristics to consider them as blood biomarkers for cancer detection and they are currently being investigated as potential diagnostic tools in multiple cancer types. Some reports have described the use of autoantibodies for early and preclinical detection of cancer, such as lung [10,11] or breast cancer [12]. The analysis of autoantibodies offers significant benefits when compared to direct determination of protein antigens associated to the tumor. Whereas detection of directly tumor-shed proteins in serum may be challenging due to their low abundance or to the difficulty of identifying simple mutations or structural modifications, serum autoantibodies are highly stable biomolecules and are produced in large quantities even after stimulation by a minimal amount of tumor antigen [12,13]. As a result, TAA-specific serum autoantibodies can constitute excellent circulating reporters for early and preclinical cancer diagnosis [14,15]. In the particular case of colorectal cancer, over 100 individual TAAs have been identified as target for autoantibody production, including full-length proteins, peptides, phage-peptides or glyco-peptides [14,16-18]. Current efforts in CRC research are directed not only to define specific TAA panels but also to develop efficient and highly sensitive analytical methods capable of detecting TAA autoantibodies in serum with optimum accuracy and reliability [19,20]. Most commonly employed methodologies are based on ELISA or protein microarrays [21] which are usually aimed at finding relative cut-off values, so far providing qualitative or semi-quantitative results. Optical biosensors can offer a valuable alternative in terms of time and sample consumption and can provide accurate quantification, which may result useful from a diagnosis point of view. Photonic and plasmonic biosensors in particular have shown great promise for the development of high-throughput and miniaturized platforms capable of carrying out label-free and highly sensitive biochemical analysis [22,23].

In this paper, we show the design and optimization of a nanoplasmonic-based biosensor for the direct detection and quantification of specific CRC-related TAA autoantibodies. We employ a refractometric nanoplasmonic biosensor whose configuration is based on the Localized Surface Plasmon Resonance (LSPR) of gold nanodisks [24]. The gold nanodisks are fabricated by hole-mask colloidal lithography [25] which is an easy, fast, low-cost and well-stablished methodology which

leads to reproducible results, with controlled density of disks on the surface. This device is highly sensitive to local refractive index (RI) changes occurring in close proximity to the surface of the transducer (in this case the gold nanodisks), such as the ones originated from biomolecular interactions. These RI changes can be detected as variations of the LSPR, which permits the real-time monitoring of the biorecognition events under label-free conditions. This nanoplasmonic biosensor has demonstrated excellent capabilities in terms of RI sensitivity improvement and signal-to-noise ratio enhancement, compared for instance with conventional Surface Plasmon Resonance [26] and more specifically its performance has also been validated for accurate detection of clinical biomarkers and antibodies in blood serum in few minutes[26,27]. The proposed biosensor strategy would allow rapid and simple analysis of TAA autoantibodies, providing a unique and innovative tool for CRC diagnosis.

2. Experimental

2.1. Materials

Main chemical reagents and salts for buffer preparation and biofunctionalization procedure were acquired from Sigma-Aldrich (Germany): alkanethiols for self-assembled monolayer (SAM) formation (16-mercaptohexadecanoic acid (MHDA) and 11-mercaptoundecanol (MUOH)), reagents for carboxylate group activation (1-ethyl-4(3-dimethylaminopropyl)carbodiimide hydrochloride (EDC) and N-hydroxysulfosuccinimide (s-NHS)), ethanolamine and Tween 20. Poly-L-Lysine-graft-PEG (MW~70000 $g \cdot mol^{-1}$ was purchased to SuSoS (Switzerland). Commercial serum was obtained from Sigma-Aldrich (Germany) and commercial plasma was purchased to Innovative Research (USA). cDNA encoding for full-length human genes EDIL3 and GTF2B in pDONR221 were obtained from the PlasmId repository (Harvard Institute of Proteomics) and, then, subcloned into pET28a (Novagen) for protein expression. TAAs were expressed in bacteria and purified according to previous studies [16,28]. The Institutional Ethical Review Boards of the Centro de Investigaciones Biológicas (CIB), the Spanish National Research Council (CSIC) and Hospital de Cabueñes (Gijón) approved this study on biomarker discovery in colorectal cancer. Serum samples were obtained from

the Hospital of Cabueñes previous informed consent of the patients. Antibodies anti-GTF2b and anti-EDIL3 were purchased to Santa Cruz Biotechnology (USA) and Abcam (UK), respectively.

2.2. Description of the Nanoplasmonic Biosensor

The nanoplasmonic device is based on a recently implemented LSPR sensing scheme based on a waveguided electromagnetic mode that arises in thin monolayers of sparse and randomly distributed plasmonic nanoparticles. Nanoplasmonic chips consist of short-range ordered arrays of gold nanodisks (diameter D = 100 nm, height H = 20 nm (Ti/Au 1/19 nm), surface density F = 6-7%) fabricated by hole-mask colloidal lithography (HCL) on glass substrates [25]. A detailed description of the fabrication process has been included in the Supplementary Material. Sensor chips are clamped between a trapezoidal glass prism (n=1.52) contacting the samples through RI matching oil (n≈1.512) and a custom-made Delrin flow cell (volume=4 μL). The flow cell is connected to a microfluidic system consisting on a syringe pump (New Era, NE-1000, USA) with adjustable pumping speed that ensures a constant liquid flow and a manually operated injection valve (IDEZ Health and Science, V-451, USA). For LSPR excitation, gold nanodisks are illuminated with a collimated halogen light (HL-2000, Micro-pack, USA) set in transverse-electric (TE) polarization mode at an angle of incidence of 80°. The reflected light is collected and fiber-coupled to a CCD spectrometer (Ocean Optics, Jazz Module, US). Reflectivity spectra are acquired every 3 ms, and 300 consecutive spectra are averaged to provide the spectrum to be analyzed. Excitation at 80° results in deep reflectivity dips at $\lambda_{LSPR} \approx$ 750 nm that lead to optimal biosensor performance [24,26]. Biomolecular interactions taking place close to the gold nanodisks induce RI changes on the surface and, as a consequence, wavelength displacements ($\Delta\lambda_{LSPR}$). Tracking of the real-time resonance peak position is achieved via polynomial fit using homemade readout software.

2.3. Surface functionalization

Prior to surface functionalization, sensor chips were subjected to a cleaning procedure consisting of consecutive 1 min sonication cycles in acetone, ethanol and MilliQ water, respectively, dried with N_2 stream and placed in a UV/O_3 generator (BioForce Nanoscience, USA) for 20 min, after which they

were rinsed with ethanol and water and dried with N_2. Formation of the alkanethiol SAM was carried out by coating the chip with 250 µM MHDA in ethanol for 5h at room temperature. Then, surface was rinsed with ethanol and water and dried with N_2 stream. For the activation of the carboxylic groups, the chip was incubated with 0.2 M EDC/0.05 M s-NHS in MES buffer (0.1 M pH 5.5) for 20 min at RT and then rinsed with water and dried. The surface was then immediately immersed in the TAA solution in PBS (10 mM pH 7.4) and incubated overnight at 4°C. Finally, biofunctionalized sensors were carefully rinsed with PBS and water, dried with N_2 stream and mounted in the platform. The non-sensing glass areas were subsequently coated with PLL-g-PEG (0.5 $mg \cdot mL^{-1}$) to avoid non-specific adsorptions. Figure S3 in Supplementary Material summarizes the biofunctionalization protocol.

2.4. Antibody detection assays

For antibody analysis, PBST 0.5% (PBS + 0.5% Tween 20) was settled as running buffer. Different concentrations of specific antibody were diluted in PBST 0.5% or in commercial serum/plasma and flowed over the functionalized surface at 25 $\mu L \cdot min^{-1}$ (See Figure S9 for an example of real time senrograms for the detection of specific antibodies at different concentrations). Regeneration of the surface was achieved by injecting 20 mM NaOH at 65 $\mu L \cdot min^{-1}$. Calibration curves were fitted to a saturation total binding model. Limit of detection (LoD) was calculated as the concentration corresponding to the blank signal plus three times its standard deviation (SD), while limit of quantification (LoQ) was determined as the concentration corresponding to the minimum measurable signal, set as the blank signal plus 10 times SD. Data analysis was performed using Origin Pro software. ELISA was carried out as previously described [16,28]. Briefly, microtiter plates (Maxisorp, Nunc) were coated overnight with 0.3 µg of the purified recombinant proteins, using GST and human Annexin IV as negative controls in 50 µl of PBS. After washing three times with PBS, plates were blocked with 3% skimmed milk in PBS (MPBS) for 2 h at room temperature. Then, serum samples (dilution, 1:100 in 3% MPBS) were incubated for 2 h at room temperature. After washing, peroxidase-labeled anti-human IgG (Jackson laboratories) (dilution, 1:500 in 3% MPBS) was added for 2 h at room temperature. Then, the signal was developed with 3,3´,5,5´-tetramethylbenzidine

substrate for 10 min (Sigma-Aldrich). The reaction was stopped with 1 M HCl, and absorption measured at 450 nm.

3. Results

3.1. Description of the Nanoplasmonic Biosensor Platform

The nanoplasmonic device is based on a recently implemented LSPR sensing scheme based on a waveguided electromagnetic mode that arises in thin monolayers of sparse and randomly distributed plasmonic nanoparticles [24]. We previously reported that the in-plane LSPR excitation strongly enhances the polarizability of the nanodisks, creating an effective RI that is sufficiently large to support a guided electromagnetic mode inside the plasmonic monolayer. Both the nanoparticle surface density (F) and the incidence angle of light are key aspects that affect this sensing performance. Surface density was precisely chosen so that the optimal mode excitation (light coupling efficiency close to 100%) occurs at angles where the sensitivity was maximized (angle close to 90º). In particular we employ short-ordered arrays of gold nanodisks (diameter D = 100 nm, height H = 20 nm, surface density F = 6-7%) fabricated by hole-mask colloidal lithography (HCL) (See experimental details in Supplementary Material). This nanofabrication technique allows simple, cost-efficient and wafer-scale production of the nanoplasmonic chips. This waveguided mode results not only in a large increase of the RI sensitivity, but also strongly improves the signal-to-noise ratio. Both effects assure an overall improved RI sensing performance that is up to one order of magnitude better than that of isolated non-interacting nanodisks. Thus, RI changes occurring close to the nanodisk surfaces are much easier to detect. A schematic representation of the biosensor can be seen in Figure 1a. For LSPR excitation, the nanoplasmonic chip is illuminated with a broadband polarized light at a determined angle of incidence (Θ = 80°) [24,26], and the reflected light is collected with a spectrophotometer. The obtained spectra show a deep reflectivity dip at $\lambda_{LSPR} \approx 750$. Biomolecular interactions occurring on the nanodisks surfaces generate RI changes that, in turn, cause displacements of the spectral LSPR peak ($\Delta\lambda_{LSPR}$) (red shifts when binding occurs and blue shifts during a desorption process). The real-time interrogation of this $\Delta\lambda_{LSPR}$ enables the extraction of

quantitative information related to the biomolecular interactions taking place in a label-free manner (Figure 1.B). In addition, the designed optical platform has very small dimensions (all optical components are mounted on a 20 x 20 cm^2 portable breadboard), exemplifying its facile miniaturization and potential portability.

3.2. Design and Optimization of the Sensor Biofunctionalization

Among the numerous TAAs defined for colorectal cancer [18], we selected GTF2b (general transcription factor IIB) and EDIL3 (EGF-like repeats and discoidin I-like domain 3 protein) since both proteins have been previously evaluated as possible TAA targets for autoantibody production in colorectal cancer [14]. A study performed in cancer-induced animals provided evidences of immediate production of GTF2b and EDIL3 autoantibodies, among others [14]. The presence of autoantibodies was detectable at a very early stage in tumor development, even before adenoma formation. Especially, GTF2b could be detected before clinically observable symptomatology while EDIL3 is characterized by a more homogeneous but late response. This makes GTF2B more appropriate to enhance sensitivity while EDIL3 would enhance specificity.

In order to directly detect the autoantibodies for these two TAA, a biosensing strategy based on the direct immobilization of the TAA on the surface of the gold nanodisks has been addressed. A schematic representation of the proposed biosensor strategy is showed in Figure 1C. Biofunctionalization of the nanoplasmonic sensor chip was based on the formation of a functional alkanethiol self-assembled monolayer (SAM) specifically onto the gold nanodisks *via* thiol chemisorption, which act as linker for the covalent attachment of the antigens. We employed 16-mercaptohexadecanoic acid (MHDA) to create a tight and uniform SAM where the carboxylic groups of the MHDA are activated to readily react with lysine (Lys) residues available in the proteins. The reaction generates an amide bond between the protein and the SAM. The grafting density of antigen molecules on the surface can also be controlled by introducing a lateral spacer during the formation of the SAM (i.e. 11-mercaptoundecanol, MUOH). In parallel, glass substrate was coated with the copolymer poly-L-lysine PEG (PLL-g-PEG 0.5 $mg \cdot mL^{-1}$) to prevent and minimize possible undesired

adsorptions. The PLL-g-PEG coating generates a highly hydrophilic layer that has demonstrated to effectively reduce nonspecific binding of proteins and other compounds present in biological matrices. This step facilitates the direct measurement in these biological fluids when using label-free biosensors [26,29].

To establish the best immobilization conditions for both TAAs, the nanoplasmonic chips were independently biofunctionalized with recombinant human GTF2b and EDIL3 proteins employing different molar ratios of mixed alkanethiol SAM (MHDA/MUOH 1:0, 1:1, 1:10) at a total thiol concentration of 250 μM. The immobilization procedure was carried out *in situ* over the SAM-functionalized chip already mounted on the sensor platform, by flowing the protein solution and monitoring the covalent coupling process (Figure S4 in Supplementary Material). We compared the immobilization signals obtained with a fixed protein concentration (50 $\mu g \cdot mL^{-1}$) over the different SAM ratios. We selected 50 $\mu g \cdot mL^{-1}$ based on preliminary experiments performed with a conventional SPR biosensor. We observed that although higher concentrations of protein (i.e. 100 $\mu g \cdot mL^{-1}$) rendered higher immobilization signal, the subsequent detection of the autoantibody (at a fixed concentration of 1 $\mu g \cdot mL^{-1}$) remained similar to the one obtained with a protein concentration of 50 $\mu g \cdot mL^{-1}$ (see Figure S5 in the Supplementary Material). This was indicative of a more optimum coverage of the surface for detection purposes with 50 $\mu g \cdot mL^{-1}$ than with 100 $\mu g \cdot mL^{-1}$. Based on these results and on previous conditions optimized for protein attachment to SAMs [27] we selected 50 $\mu g \cdot mL^{-1}$ of protein for further experiments. The highest amount of protein was attached to the sensor surface when maximum carboxylic density was employed (Figure S6a in Supplementary Material), inducing wavelength shifts around 3 nm. This was observed for both GTF2b and EDIL proteins. Introduction of spacer molecules (MUOH) to the SAM resulted in lower signals thereby indicating less amount of TAA immobilized. However, the optimum TAA layer, which will lead to better detection levels, does not necessarily require maximum coverage with proteins. The appropriate distribution of antigens on the surface reveals itself as an important factor to favor the accessibility of antibodies. Control of the spacing between TAA molecules can *a priori* modulate possible steric hindrance effects and improve the ability of the antibodies to interact. We evaluated the detection

efficiency by flowing a 1 µg·mL^{-1} specific antibody solution over the corresponding GTF2b and EDIL3 functionalized surfaces. This concentration was selected for screening purposes in order to choose the best immobilization conditions before performing a full calibration curve. In addition, TAA immobilization procedure was also carried out *ex situ*, by coating the functionalized sensor chip with the protein overnight, rinsing it with buffer and then installing the protein-modified chip in the biosensor. The antibody detection signal achieved for both *ex situ* and *in situ* procedures carried out with mixed alkanethiol SAMs at different molar ratios was compared and is summarized in the Figure S6b in the Supplementary Material). No steric hindrance effects appeared to be relevant for the concentration of TAA tested (50 µg·mL^{-1}) as maximum antibody detection was obtained in all cases when maximum carboxylic density was used (MHDA/MUOH 1:0). This suggests that the immobilization of TAAs at the selected concentration on alkanethiol SAMs formed exclusively with MHDA actually provides highly efficient bioreceptor layers, as also previously reported [30]. It can also be appreciated that *ex situ* immobilization resulted in significant higher antibody signals for the same concentration of immunoreagents. This could be attributed to a more efficient coupling yield and also to a more efficient protein rearrangement on the surface facilitated by longer reaction times (protein coupling overnight *vs.* 30 min when it is done *in situ*). From the above results, overnight immobilization of TAA over a 100% MHDA SAM was selected as optimum biofunctionalization strategy for further experiments. Regeneration for a potential reutilization of the TAAs functionalized surfaces was also evaluated. For both TAA-modified surfaces – GTF2b and EDIL3 – basic conditions (20 mM NaOH) disrupted the TAA-antibody interaction without altering or modifying the immobilized proteins (Figure S7 and S8 in Supplementary Material). Under these conditions it was possible to reuse the functionalized surface with good repeatability for up to 100 cycles before progressive decrease of the antibody detection signals.

Calibration curves for both anti-GTF2b and anti-EDIL3 (Figure 2A and 2B) were then performed in standard buffer conditions (i.e. PBS with 0.5% of Tween 20 (PBST)), which according to previous works helped drastically reduce nonspecific adsorptions onto the sensor chip) [26,27]. Different antibody concentrations ranging from 50 ng·mL^{-1} to 1 µg·mL^{-1} were flowed by triplicate through the

specific TAA functionalized surfaces, respectively, and the resonance shift was obtained (Figure 2A and 2B). Limits of detection (LoD) were determined as the minimum antibody concentrations that provide an observable signal (i.e. blank signal plus 3 times its standard deviation). The LoD for anti-GTF2b assay was 10 $ng \cdot mL^{-1}$ (66 pM) and 5 $ng \cdot mL^{-1}$ (33 pM) for anti-EDIL3 assay. Limits of quantification (LoQ) were determined as the minimum measurable signal, being 34 $ng \cdot mL^{-1}$ (227 nM) and 19 $ng \cdot mL^{-1}$ (127 pM) for GTF2b and EDIL3, respectively. Besides, the specificity of the assays was confirmed by using nonspecific antibodies as control. Measurements of anti-GTF2b over an EDIL3-functionalized surface and *vice versa* led to negligible signals (Figure 2A and 2B, red lines), which corroborates the signal contribution solely comes from the specific antibody recognition and confirms the feasibility of the methodology for antibody quantification. Excellent reproducibility and stability of the biosensor-based assays were finally demonstrated by performing intra- and inter-assays (curves performed in the same nanodisk-functionalized surface and in different surfaces, respectively). As it can be seen in Table 1, the coefficient of variation (CV) for both GTF2b and EDIL3 was below the maximum variability recommended for clinical analysis (~15%) [31], both for the LoD and for the maximum signal (S_{max}), taken at the maximum antibody concentration tested ([Ab] = 1 $\mu g \cdot mL^{-1}$).

3.3. Analysis of TAA Antibodies in Serum and Plasma

In order to evaluate the influence of the matrix, commercial serum (undiluted, and diluted 1:1 and 1:10 in PBST) and commercial plasma (undiluted, and diluted 1:1 and 1:10 in PBST) were flowed over the biofunctionalized nanoplasmonic surfaces (i.e. TAA layer + PLL-g-PEG coating) (Figure 3). As it can be seen in the sensorgrams, in both cases a significant background signal was observed due to the binding of fluid components onto the bioactive layer, being slightly higher for undiluted plasma (whose difference compared to serum is the presence of fibrinogen). A 1:10 dilution in PBST was necessary to achieve a complete reduction of nonspecific adsorptions for both fluids, resulting in virtually no background signals.

Besides the influence of the nonspecific binding onto the surface, possible matrix effects on the interaction of the antibody with the TAA-coated layer can occur, altering the analysis features. In order to assess this undesired effect, both GTF2b and EDIL3 calibration curves were obtained by spiking serum or plasma with several known concentrations of antibodies and then diluting them in PBST (1:10) (Figure 4). The curves were analogous to those obtained with standard buffer conditions although a slight increase of the LoDs was observed. This minor worsening can be attributed to a possible hindrance of the antibody/TAA interaction. For the GTF2b antibody, the LoD was 16 $ng \cdot mL^{-1}$ in diluted serum and 15 $ng \cdot mL^{-1}$ in diluted plasma, compared to a LoD of 10 $ng \cdot mL^{-1}$ in buffer. In the case of EDIL3 antibody detection, LoDs were 12 $ng \cdot mL^{-1}$ in diluted serum and 11 $ng \cdot mL^{-1}$ in diluted plasma, compared to 5 $ng \cdot mL^{-1}$ in buffer. Overall the sample dilution (1:10) has inevitably decreased the sensitivity over one order of magnitude, with detectabilities around 150-160 $ng \cdot mL^{-1}$ for GTF2b and around 110-120 $ng \cdot mL^{-1}$ for EDIL3, respectively depending on the fluid.

Clinical serum samples from CRC patients were analyzed with the nanoplasmonic biosensor for a preliminary assessment of the viability of our approach. Serum samples collected from patients from the Hospital of Cabueñes (Gijón, Spain) with diagnosed CRC and samples from healthy individuals were evaluated employing the optimal conditions selected before (1:10 dilution with PBST). All samples were previously analyzed for the presence of GTF2b autoantibodies using semi-quantitative ELISA, so the absolute concentration of the target biomarker was unknown. Table 2 compares the concentration values obtained with the nanoplasmonic biosensor (in $\mu g \cdot mL^{-1}$) to absorbance values (in optical density units, OD) obtained with the ELISA (quantitative data is not commonly determined with the ELISA for autoantibodies). A consistent correlation was observed in terms of relative signals. Negative samples from healthy subjects resulted below the LoD established for our biosensor technique (160 $ng \cdot mL^{-1}$) while positive samples lead to relatively high signals (i.e. high concentration of GTF2b autoantibodies).

4. Discussion

A major challenge in colorectal cancer research focuses on the development of novel diagnostic techniques for simple, rapid and accurate detection of the disease at earlier stages. In this regard,

cancer-associated autoantibodies generated by the immune system during tumor appearance have evidenced its high value as blood-circulating biomarkers for preclinical cancer diagnosis. We propose the use of an innovative nanoplasmonic biosensor for the direct and label-free quantification of CRC autoantibodies in serum or plasma. Our nanoplasmonic biosensor offer real-time detection of TAA antibodies without the need of any labels or sample pretreatments, which simplifies the analysis and provides interesting alternatives to develop small, fast and user-friendly point-of-care (POC) devices that could be used directly at doctor's office. The implementation of POC biosensors for rapid and reliable CRC screening could substantially afford a breakthrough towards non-invasive and highly specific diagnostic tools for this disease which in turn would help to improve patient survival rates.

The overall performance of the biosensor assay has been demonstrated for the determination of autoantibodies against two important CRC antigens: GTF2b and EDIL3. Both autoantibodies were selected as representative for the disease as they are generated at very early stages of CRC development and can be detected in blood serum before the onset of tumor lesions [14]. Biofunctionalization of the nanoplasmonic sensors has been designed to create a highly stable TAA layer that ensures an efficient capture of the specific antibodies. The immobilization strategy is based on the material-selective functionalization of the gold nanodisks through the formation of an alkanethiol SAM, which guarantees the biomolecular interaction to take place solely on the sensor spots. The PLL-g-PEG coating of the glass areas (which represents over the 94% of the surface) prevents the nonspecific binding to substrate. The covalent coupling of the TAA *via* the terminal amine groups of Lys residues is a simple and robust procedure that can be applied to immobilize virtually all proteins. Several biofunctionalization conditions have been optimized (e.g. alkanethiol SAM ratios, binding time, etc.) for the enhancement of the antibody capture efficacy reaching a LoD of 10 $ng \cdot mL^{-1}$ (~ 66 pM) for GTF2b antibody and 5 $ng \cdot mL^{-1}$ (~ 33 pM) for EDIL3 antibody in standard buffer, showing in both cases high selectivity and reproducibility. A complete assay cycle (including regeneration) is accomplished in 30 min. Besides, the bioactive surface with the immobilized TAA has proven to be reusable for more than 100 cycles with good repeatability.

An ultimate goal in POC development relies on the ability to readily detect the biomarkers in biological fluids. Here, we have exploited the unique hydrophilic properties of the PLL-g-PEG coating layer together with the use of a dilution buffer containing a high concentration of surfactant (Tween 20) in order to minimize possible interferences coming from serum or plasma matrices. In particular, a simple dilution of the biological sample 1:10 with PBST has led to a complete removal of background signals enabling the direct quantification without requiring purification or other extra pretreatments. This dilution factor inevitably increases the limit of detection. However, it is much lower than the minimum dilution required in the ELISA assay. Overall the features of the resultant calibration curves, both in diluted serum and plasma, offer a highly reliable analysis method to quantify the TAA autoantibodies with elevated selectivity and reproducibility. Moreover, clinical samples analysis further demonstrates the potential of using this device in comparison to conventional ELISA methods, according to the good correlation observed for the detection of GTF2b antibodies in CRC-diagnosed patients and healthy individuals. In this regard, a more complete quantitative clinical validation will be required in the future. However, to our knowledge, serological concentration levels of CRC autoantibodies have not been fully established so far, as most research articles in the field especially focus on their identification and the assessment of their diagnostic and/or prognostic value. Nevertheless we cannot obviate the evident usefulness of knowing this concentration value compared with other semi-quantitative or qualitative methods, not only from a perspective of early diagnosis but also for disease follow-up. Besides, the possibility of quantifying autoantibodies concentration in serum samples may allow further comprehension of the humoral response triggered by the tumor and harness the basis for the improvement of prognosis of the disease. On-going work currently focuses on the improvement of biofunctionalization strategies and the use of antifouling agents that permit direct measurements of undiluted serum and plasma, therefore enhancing the detectability at least 10-fold. Moreover, the biofunctionalization methodology developed can be easily adjusted for any TAA with potential interest. This facilitates the eventual expansion of the biosensor strategy to elaborate a multiplexed compact analytical platform for the simultaneous detection of a CRC-specific panel of autoantibodies, which is ultimately necessary to fully cover the patient variability and to maximize the sensitivity and specificity of the method.

5. Conclusions

We have developed a novel analytical label-free strategy for the detection of tumor-associated autoantibodies in blood serum and plasma based on an innovative nanoplasmonic biosensor technology. This strategy could provide a reliable and non-invasive screening and diagnosis of colorectal cancer at early stages. Our biosensor allows the label-free quantification of specific CRC-related autoantibodies in few minutes, without requiring any sample purification or pretreatment. Several biofunctionalization parameters have been optimized, reaching a limit of detection of 1 nM (150-160 $ng \cdot mL^{-1}$) for direct measurements in human serum or plasma. Selectivity and reproducibility of the assay have been also evaluated demonstrating the excellent accuracy and robustness of the biosensor. The analysis of clinical samples from colorectal cancer patients has shown good correlation with ELISA. Overall, the results obtained highlight the exceptional potential of our nanoplasmonic biosensor as a tool for the early detection of colorectal cancer and current efforts are focused on establishing a multiplexed approach to expand the strategy to a CRC-panel of autoantibodies.

Acknowledgements

M. Soler acknowledges financial support from "Programa de Formación de Personal Investigador (FPI)" from the Spanish Ministry of Economy and Competitiveness (MINECO). R. Villar-Vazquez was a recipient of a FPU fellowship from the Spanish Ministry of Education and Culture. We acknowledge the financial support from COLONTEST project (RETOS-COLABORACIÓN Subprogram, RTC-2014-1518-1). The NanoB2A is a consolidated research group (Grup de Recerca) of the Generalitat de Catalunya and has support from the Departament d'Universitats, Recerca i Societat de la Informació de la Generalitat de Catalunya (2014 SGR 624). ICN2 is the recipient of Grant SEV-2013-0295 from the "Severo Ochoa Centers of Excellence" Program of Spanish MINECO. In addition, JI Casal was supported by the grant BIO2012-31023 from the MINECO.

References

[1] A. Jemal, F. Bray, M.M. Center, J. Ferlay, E. Ward, D. Forman, Global cancer statistics, CA Cancer J. Clin. 61 (2011) 69-90.

[2] F.A. Haggar, R.P. Boushey, Colorectal cancer epidemiology: incidence, mortality, survival, and risk factors, Clin. Colon Rectal Surg. 22 (2009) 191.

[3] S. Winawer, R. Fletcher, D. Rex, J. Bond, R. Burt, J. Ferrucci, T. Ganiats, T. Levin, S. Woolf, D. Johnson, Colorectal cancer screening and surveillance: clinical guidelines and rationale—update based on new evidence, Gastroenterology 124 (2003) 544-560.

[4] B.-A. Adelstein, P. Macaskill, S.F. Chan, P.H. Katelaris, L. Irwig, Most bowel cancer symptoms do not indicate colorectal cancer and polyps: a systematic review, BMC Gastroenterol. 11 (2011) 65-65.

[5] M. Duffy, A. Van Dalen, C. Haglund, L. Hansson, E. Holinski-Feder, R. Klapdor, R. Lamerz, P. Peltomaki, C. Sturgeon, O. Topolcan, Tumour markers in colorectal cancer: European Group on Tumour Markers (EGTM) guidelines for clinical use, Eur. J. Cancer 43 (2007) 1348-1360.

[6] N. The Cancer Genome Atlas, Comprehensive Molecular Characterization of Human Colon and Rectal Cancer, Nature 487 (2012) 330-337.

[7] C.A. Casiano, M. Mediavilla-Varela, E.M. Tan, Tumor-associated antigen arrays for the serological diagnosis of cancer, Mol. Cell. Proteomics 5 (2006) 1745-1759.

[8] W. Liu, B. Peng, Y. Lu, W. Xu, W. Qian, J.-Y. Zhang, Autoantibodies to tumor-associated antigens as biomarkers in cancer immunodiagnosis, Autoimmun Rev 10 (2011) 331-335.

[9] S. Kobold, T. Lütkens, Y. Cao, C. Bokemeyer, D. Atanackovic, Autoantibodies against tumor-related antigens: incidence and biologic significance, Hum. Immunol. 71 (2010) 643-651.

[10] P. Boyle, C. Chapman, S. Holdenrieder, A. Murray, C. Robertson, W. Wood, P. Maddison, G. Healey, G. Fairley, A. Barnes, Clinical validation of an autoantibody test for lung cancer, Ann. Oncol. 22 (2011) 383-389.

[11] J. Qiu, G. Choi, L. Li, H. Wang, S.J. Pitteri, S.R. Pereira-Faca, A.L. Krasnoselsky, T.W. Randolph, G.S. Omenn, C. Edelstein, Occurrence of autoantibodies to annexin I, 14-3-3 theta and LAMR1 in prediagnostic lung cancer sera, J. Clin. Oncol. 26 (2008) 5060-5066.

[12] C. Chapman, A. Murray, J. Chakrabarti, A. Thorpe, C. Woolston, U. Sahin, A. Barnes, J. Robertson, Autoantibodies in breast cancer: their use as an aid to early diagnosis, Ann. Oncol. (2007).

[13] Y. Hosono, M. Goto, D. Kobayashi, K. Kuribayashi, M. Tanaka, N. Watanabe, Diagnostic relevance of autoantibody detection against inhibitors of apoptosis proteins in colon cancer and colon adenoma, Mol. Clin. Oncol. 3 (2015) 595-600.

[14] R. Barderas, R. Villar-Vazquez, M.J. Fernandez-Acenero, I. Babel, A. Pelaez-Garcia, S. Torres, J.I. Casal, Sporadic colon cancer murine models demonstrate the value of autoantibody detection for preclinical cancer diagnosis, Sci. Rep. 3 (2013) 2938.

[15] Y.S. Cho-Chung, Autoantibody biomarkers in the detection of cancer, BBA-Mol Basis Dis 1762 (2006) 587-591.

[16] I. Babel, R. Barderas, R. Diaz-Uriarte, V. Moreno, A. Suarez, M.J. Fernandez-Acenero, R. Salazar, G. Capella, J.I. Casal, Identification of MST1/STK4 and SULF1 proteins as autoantibody targets for the diagnosis of colorectal cancer by using phage microarrays, Mol. Cell. Proteomics 10 (2011) M110 001784.

[17] R. Barderas, I. Babel, R. Diaz-Uriarte, V. Moreno, A. Suarez, F. Bonilla, R. Villar-Vazquez, G. Capella, J.I. Casal, An optimized predictor panel for colorectal cancer diagnosis based on the combination of tumor-associated antigens obtained from protein and phage microarrays, J. Proteomics 75 (2012) 4647-55.

[18] H. Chen, S. Werner, S. Tao, I. Zörnig, H. Brenner, Blood autoantibodies against tumor-associated antigens as biomarkers in early detection of colorectal cancer, Cancer Lett. 346 (2014) 178-187.

[19] F.J. Lowe, W. Shen, J. Zu, J. Li, H. Wang, X. Zhang, L. Zhong, A novel autoantibody test for the detection of pre-neoplastic lung lesions, Mol. Cancer 13 (2014) 78.

[20] M. Reuschenbach, J. Dörre, T. Waterboer, J. Kopitz, M. Schneider, N. Hoogerbrugge, E. Jäger, M. Kloor, M. von Knebel Doeberitz, A multiplex method for the detection of serum antibodies against in silico-predicted tumor antigens, Cancer Immunol Immun 63 (2014) 1251-1259.
[21] P. Zaenker, M.R. Ziman, Serologic Autoantibodies as Diagnostic Cancer Biomarkers—A Review, Cancer Epidemiol. Biomarkers Prev. 22 (2013) 2161-2181.
[22] M.C. Estevez, M. Alvarez, L.M. Lechuga, Integrated optical devices for lab-on-a-chip biosensing applications, Laser Photon Rev 6 (2012) 463-487.
[23] O. Tokel, F. Inci, U. Demirci, Advances in plasmonic technologies for point of care applications, Chem. Rev. 114 (2014) 5728-5752.
[24] M.A. Otte, M.C. Estévez, D. Regatos, L.M. Lechuga, B. Sepúlveda, Guiding Light in Monolayers of Sparse and Random Plasmonic Meta-atoms, ACS Nano 5 (2011) 9179-9186.
[25] H. Fredriksson, Y. Alaverdyan, A. Dmitriev, C. Langhammer, D.S. Sutherland, M. Zäch, B. Kasemo, Hole–Mask Colloidal Lithography, Adv. Mater. 19 (2007) 4297-4302.
[26] M. Soler, et al., Highly sensitive dendrimer-based nanoplasmonic biosensor for drug allergy diagnosis, Biosens. Bioelectron. 66 (2015) 115-123.
[27] M. Soler, M.-C. Estevez, M. Alvarez, M.A. Otte, B. Sepulveda, L.M. Lechuga, Direct detection of protein biomarkers in human fluids using site-specific antibody immobilization strategies, Sensors 14 (2014) 2239-2258.
[28] I. Babel, R. Barderas, R. Díaz-Uriarte, J.L. Martínez-Torrecuadrada, M. Sánchez-Carbayo, J.I. Casal, Identification of Tumor-associated Autoantigens for the Diagnosis of Colorectal Cancer in Serum Using High Density Protein Microarrays, Mol. Cell. Proteomics 8 (2009) 2382-2395.
[29] R. Marie, A. Dahlin, J. Tegenfeldt, F. Höök, Generic surface modification strategy for sensing applications based on Au/SiO2 nanostructures, Biointerphases 2 (2007) 49-55.
[30] J.-F. Masson, T.M. Battaglia, J. Cramer, S. Beaudoin, M. Sierks, K.S. Booksh, Reduction of nonspecific protein binding on surface plasmon resonance biosensors, Anal. Bioanal. Chem. 386 (2006) 1951-1959.
[31] A. Buick, M. Doig, S. Jeal, G. Land, R. McDowall, Method validation in the bioanalytical laboratory, J. Pharm. Biomed. Anal. 8 (1990) 629-637.

Figure Captions:

Figure 1. (a) Schematic representation of the miniaturized nanoplasmonic biosensor. A picture of the nanodisks and a SEM image of the actual shape of the gold nandisks fabricated on the glass substrate are also shown. **(b)** Graphs showing the resonance peak (photon counts *vs.* λ) *(left)* and the shift of the resonance peak over time ($\Delta\lambda_{LSPR}$ *vs.* time) *(right)*; **(c)** TAA biofunctionalization methodology based on covalent coupling to an alkanethiol SAM and subsequent antibody detection.

Figure 2. (a) Calibration curve for anti-GTF2b detection performed over GTF2b-biofunctionalized nanodisks (black). Red dashed line indicates nonspecific adsorption of a control antibody (anti-EDIL3); **(b)** Calibration curve for anti-EDIL3 detection performed over EDIL3-biofunctionalized nanodisks (black). Red dashed line indicates nonspecific adsorption of a control antibody (anti-GTF2b).

Figure 3. (a) Background signal corresponding to nonspecific adsorption of undiluted serum (black), serum diluted 1:1 in PBST 0.5% (purple) and serum diluted 1:10 in PBST 0.5% (green); **(b)** Background signal corresponding to nonspecific adsorption of undiluted plasma (blue), plasma diluted 1:1 in PBST 0.5% (orange) and plasma diluted 1:10 in PBST 0.5% (pink).

Figure 4. (a) Calibration curves for anti-GTF2b antibody detection in PBST buffer (black), serum diluted 1:10 in PBST (green) and plasma diluted 1:10 in PBST (pink); **(b)** Calibration curves for anti-EDIL3 antibody detection in PBST buffer (black), serum diluted 1:10 in PBST (green) and plasma diluted 1:10 in PBST (pink).

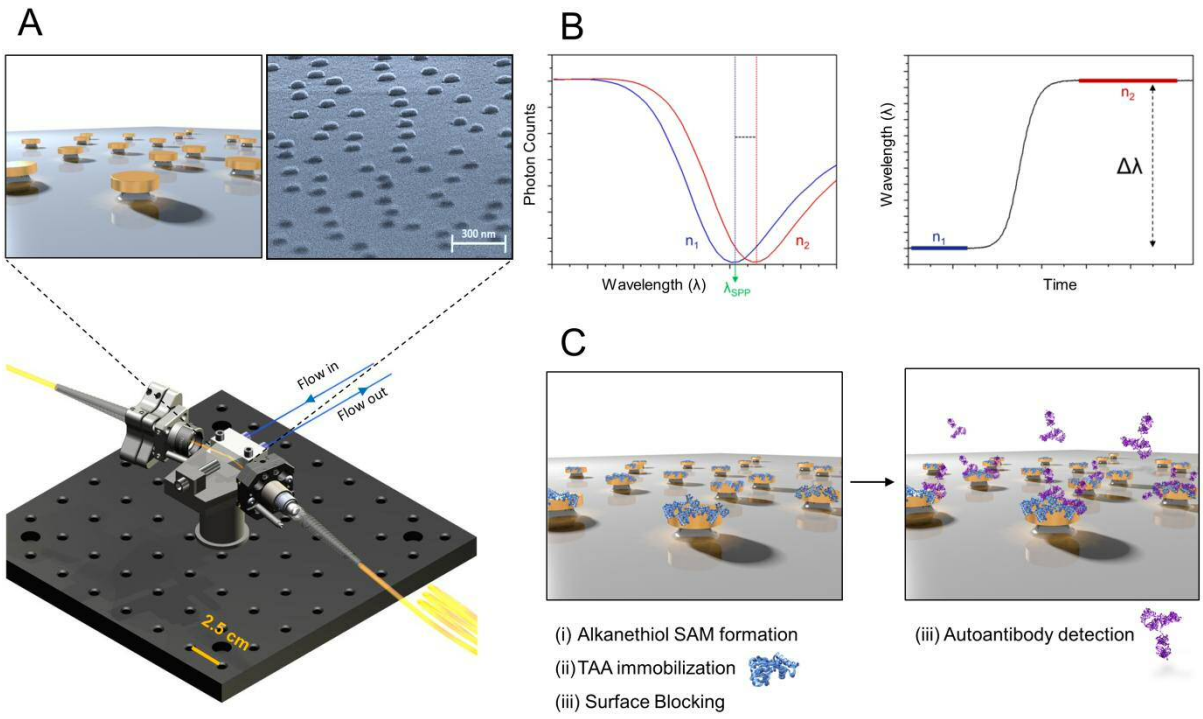
A
300 nm
Flow in
Flow out
2.5 cm
B
Photon Counts
Wavelength (λ)
λ_{SPP}
n_1
n_2
Wavelength (λ)
Time
n_1
n_2
Δλ
C
(i) Alkanethiol SAM formation
(ii) TAA immobilization
(iii) Surface Blocking
(iii) Autoantibody detection

Figure 1

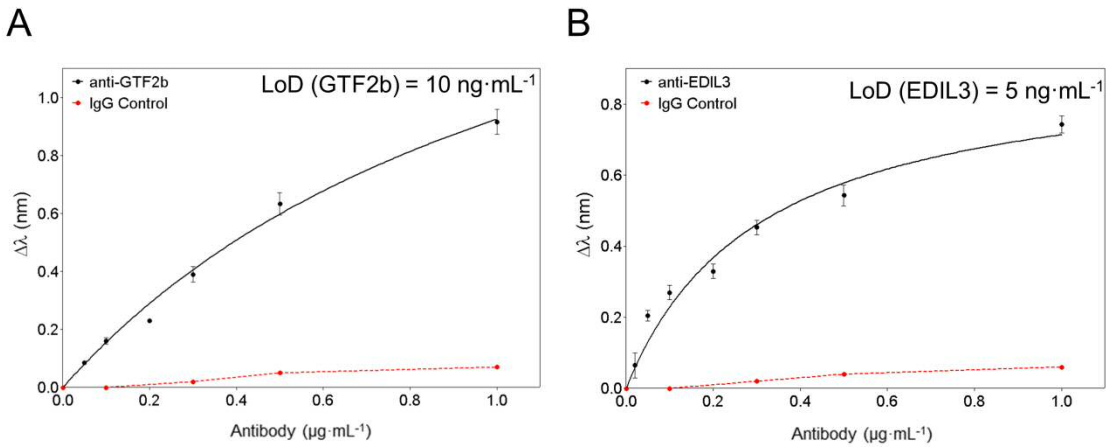
A
anti-GTF2b
IgG Control
LoD (GTF2b) = 10 ng·mL-1
Δλ (nm)
Antibody (µg·mL-1)
B
anti-EDIL3
IgG Control
LoD (EDIL3) = 5 ng·mL-1
Δλ (nm)
Antibody (µg·mL-1)

Figure 2

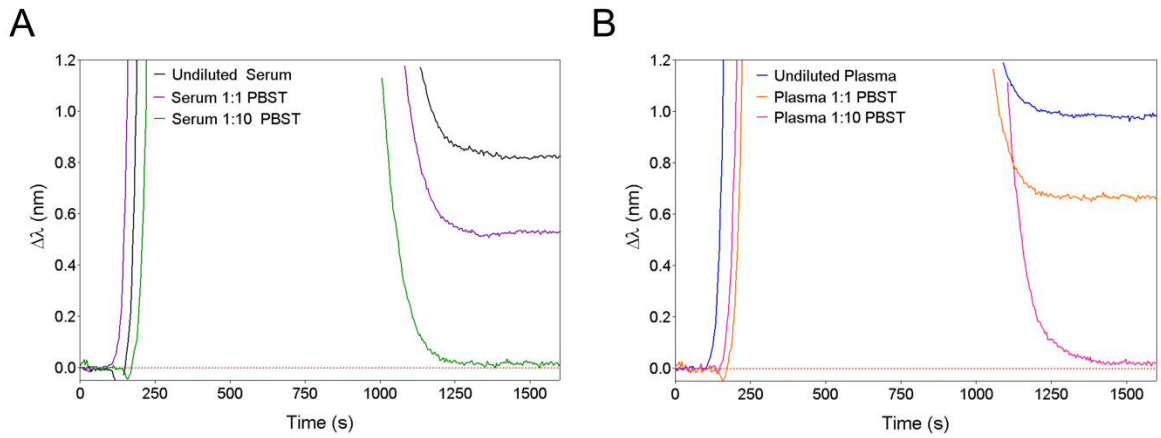
A
Undiluted Serum
Serum 1:1 PBST
Serum 1:10 PBST
Δλ (nm)
Time (s)
B
Undiluted Plasma
Plasma 1:1 PBST
Plasma 1:10 PBST
Δλ (nm)
Time (s)

Figure 3

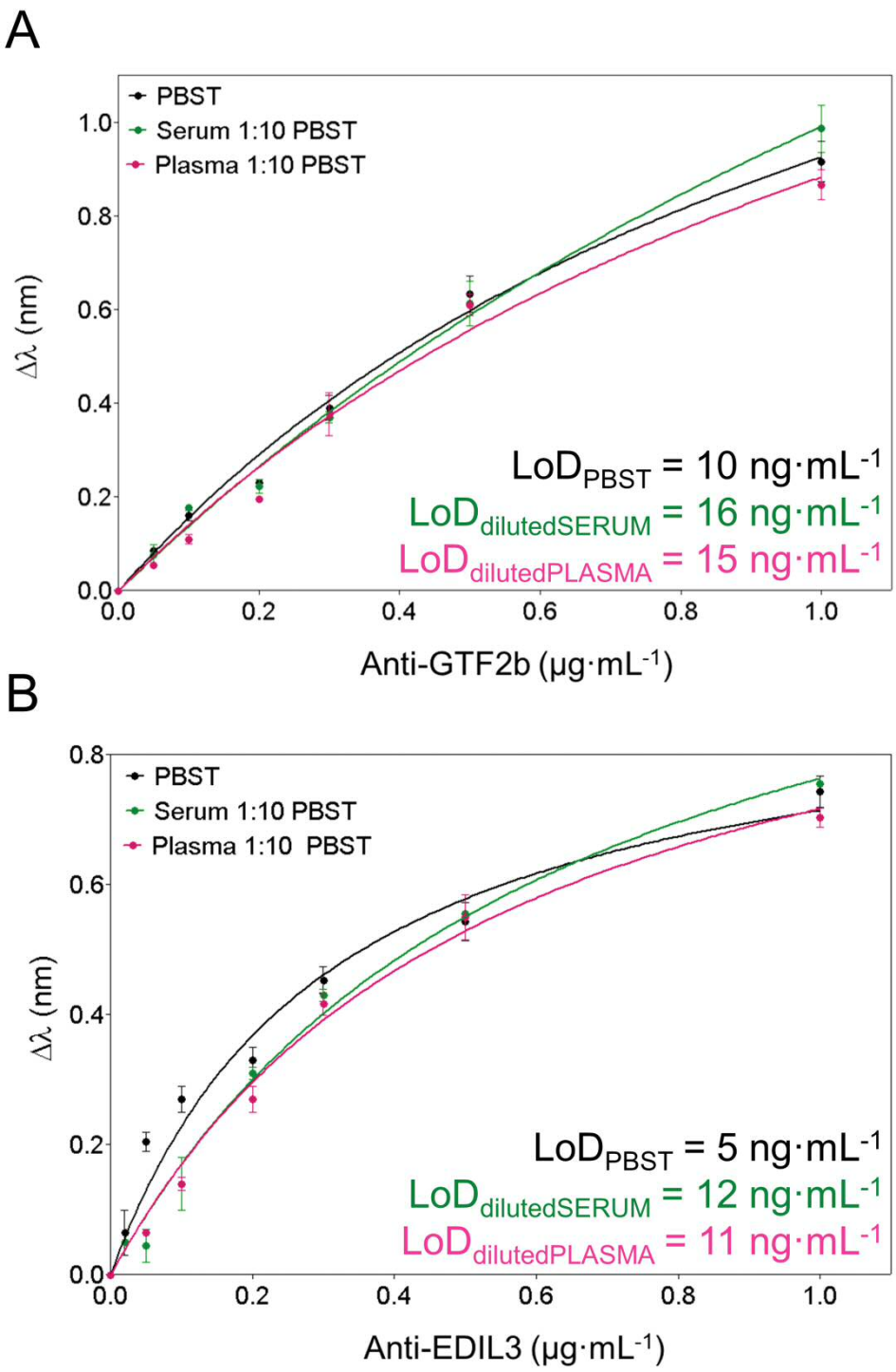
A
PBST
Serum 1:10 PBST
Plasma 1:10 PBST
Δλ (nm)
Anti-GTF2b (µg·mL-1)
LoDPBST = 10 ng·mL-1
LoDdilutedSERUM = 16 ng·mL-1
LoDdilutedPLASMA = 15 ng·mL-1
B
PBST
Serum 1:10 PBST
Plasma 1:10 PBST
Δλ (nm)
Anti-EDIL3 (µg·mL-1)
LoDPBST = 5 ng·mL-1
LoDdilutedSERUM = 12 ng·mL-1
LoDdilutedPLASMA = 11 ng·mL-1

Figure 4

Table 1. Inter and intra-assay features for GTF2b and EDIL3 antibodies detection with the nanoplasmonic biosensor

		GTF2b antibody		EDIL3 antibody	
		Mean ± SD*	**% CV**	**Mean ± SD**	**% CV**
Intra-assay	**LOD ($ng \cdot mL^{-1}$)**	9.7 ± 0.5	5.15	5.2 ± 0.2	3.77
	S_{max} (nm)	0.937 ± 0.0015	1.63	0.733 ± 0.016	2.08
Inter-assay	**LOD ($ng \cdot mL^{-1}$)**	10.1 ± 1.2	11.9	4.9 ± 0.4	8.16
	S_{max} (nm)	0.917 ± 0.07	8.19	0.743 ± 0.04	5.60

* Mean and standard deviation of 3 replicates

Table 2. Clinical serum samples analysis determined by ELISA and by the nanoplasmonic biosensor.

Sample		GTF2b Analysis Results	
		ELISA (OD)	**Nanobiosensor ($ng \cdot mL^{-1}$)***
G30	Negative	0.18	ND †
G42	Positive	0.48	175 ± 8
G56	Positive	0.56	254 ± 10
G101	Negative	0.13	ND †

***** Mean ± SD for 3 replicates

† ND: No Detected (below limit of detection: 160 $ng \cdot mL^{-1}$)

Figure 1

Click here to download high resolution image

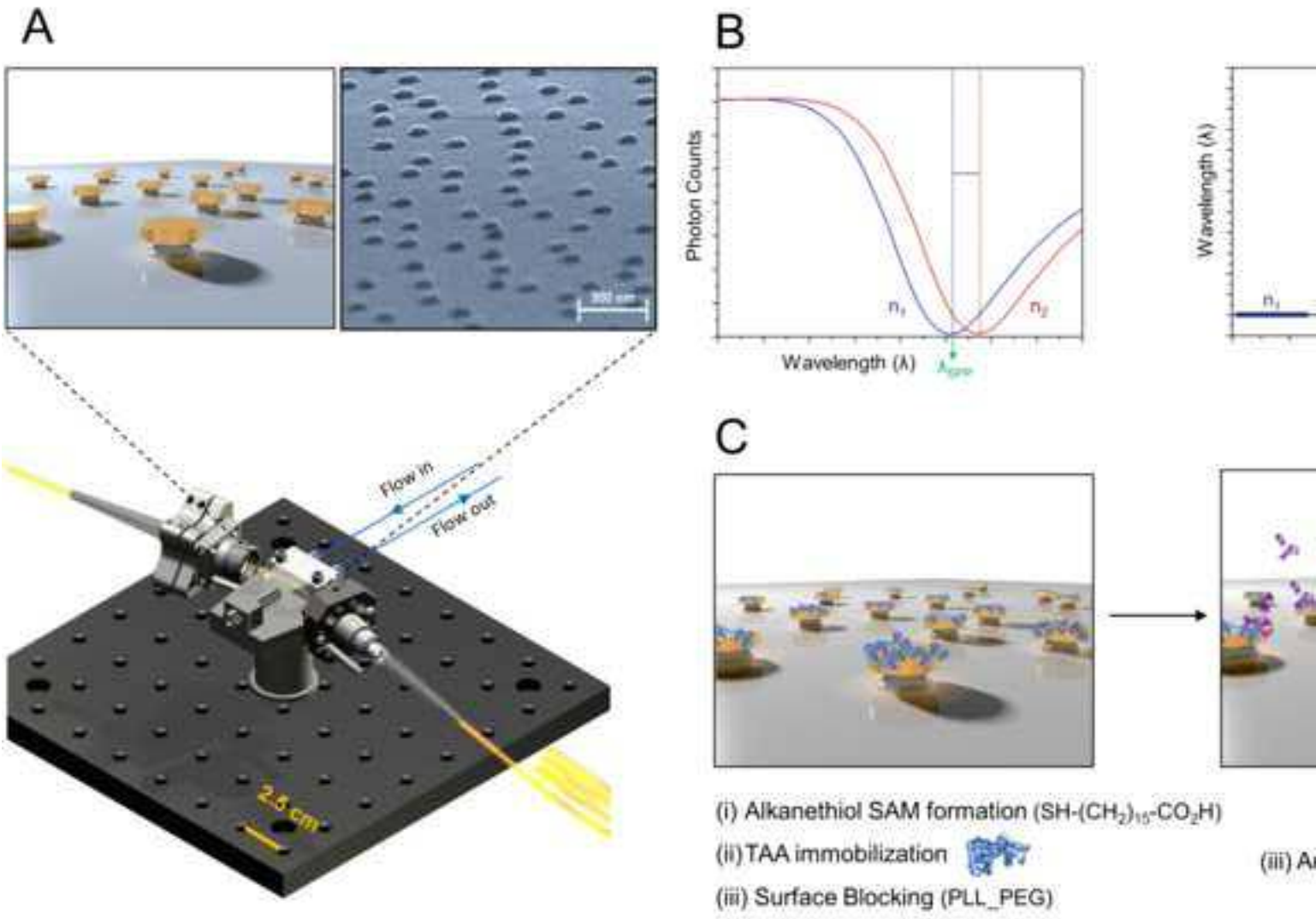

Figure 2

Click here to download high resolution image

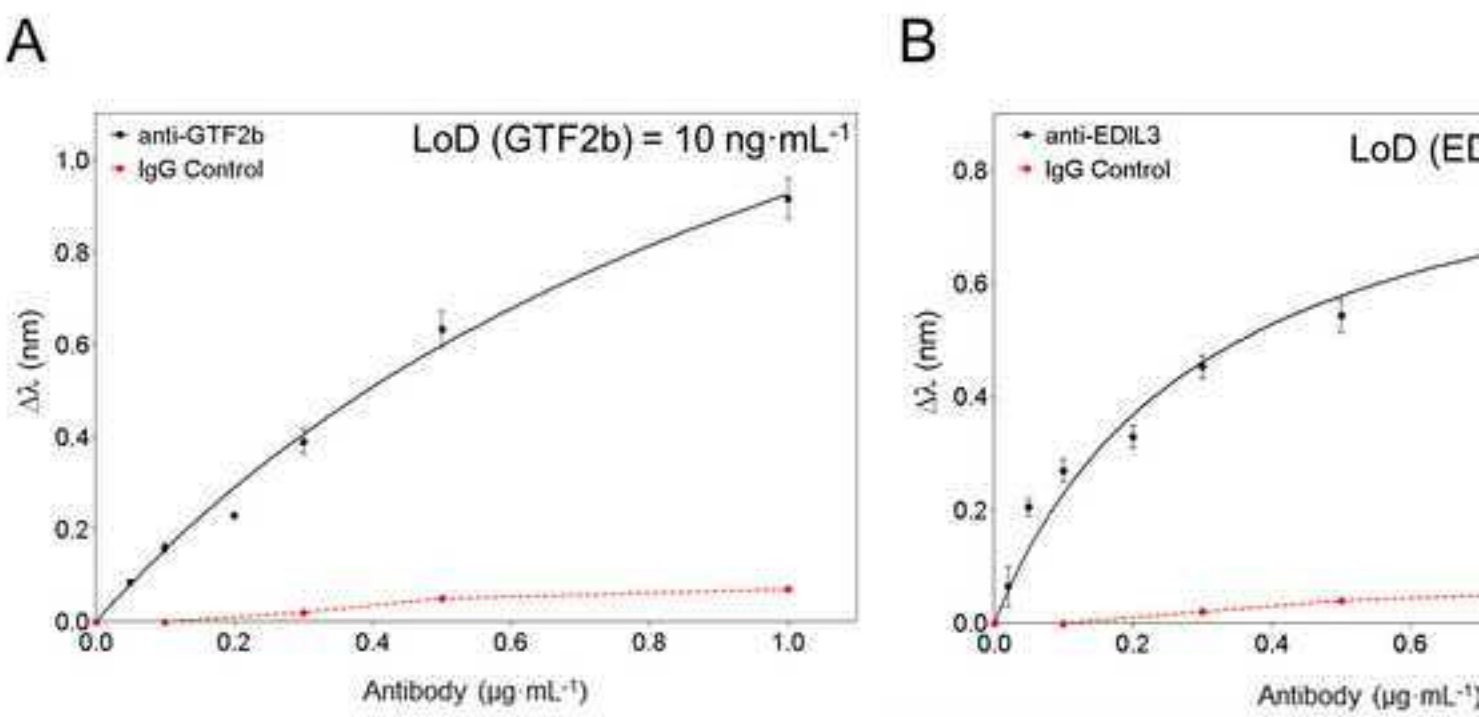

Figure 3

Click here to download high resolution image

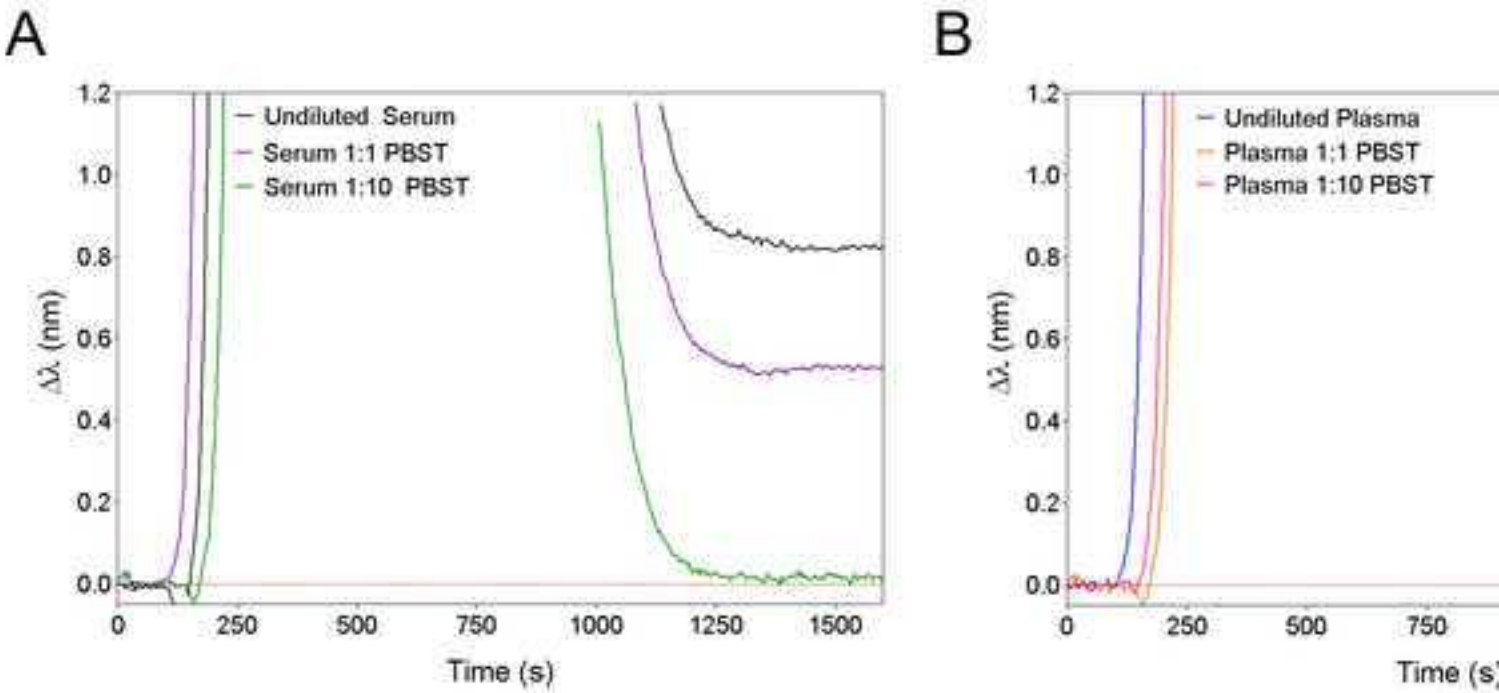

Figure 4

Click here to download high resolution image

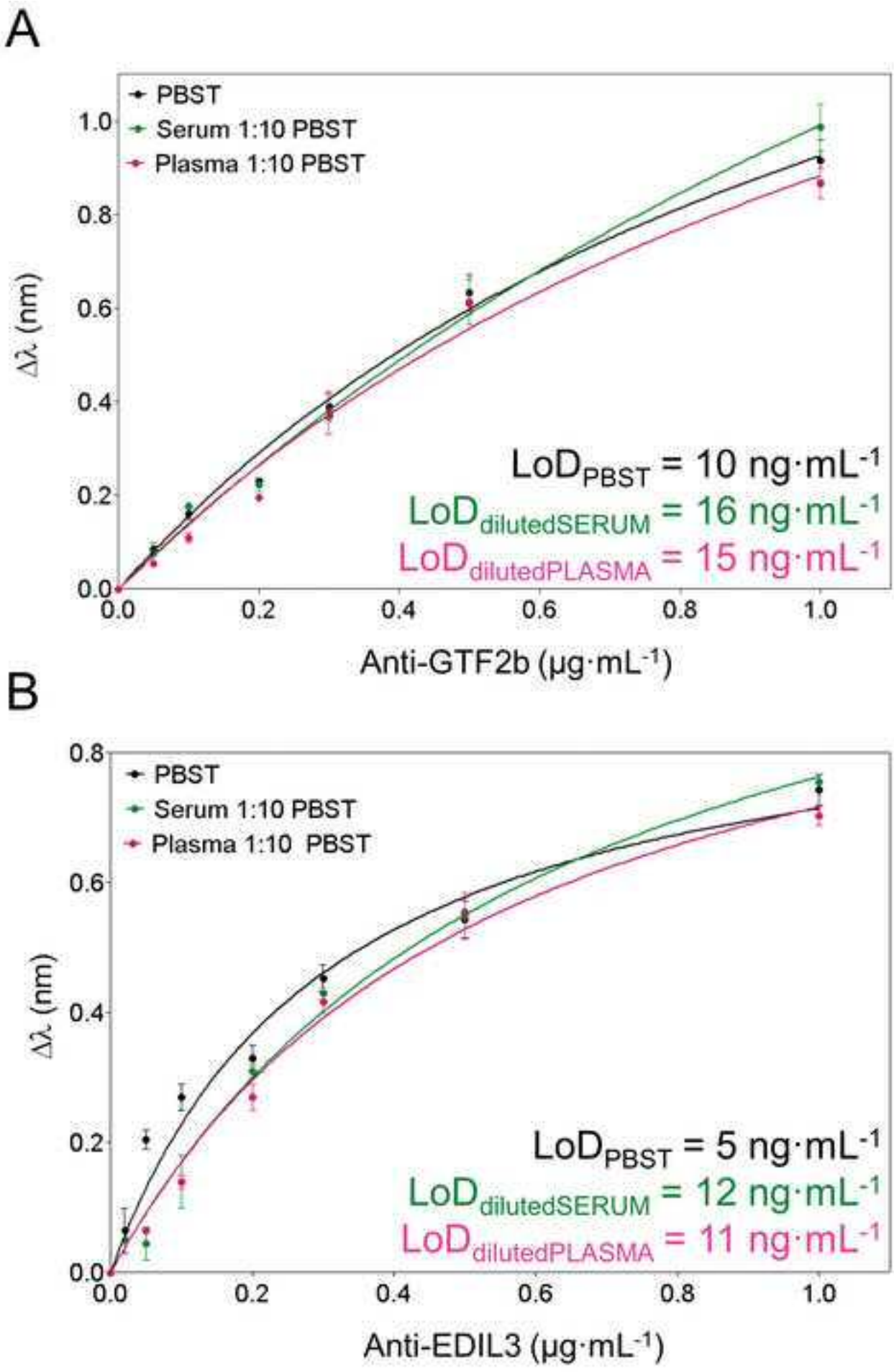

Electronic Supplementary Material (online publication only)

Click here to download Electronic Supplementary Material (online publication only): Soler_Supplementary Material.pdf

Label-free Nanoplasmonic Sensing of Tumor-Associate Autoantibodies for Early Diagnosis of Colorectal Cancer

Maria Soler[a,b,†], M.-Carmen Estevez[b,a,*], Roi Villar-Vazquez[c], J. Ignacio Casal[c] and Laura M. Lechuga[a,b]

[a]Nanobiosensors and Bioanalytical Applications Group (NanoB2A), Catalan Institute of Nanoscience and Nanotechnology (ICN2), CSIC and The Barcelona Institute of Science and Technology, Campus UAB, Bellaterra, 08193 Barcelona, Spain

[b]CIBER-BBN Networking Center on Bioengineering, Biomaterials and Nanomedicine, Spain

[c]Functional Proteomics Group, Centro de Investigaciones Biológicas (CIB-CSIC), 28040 Madrid, Spain

[†]*Present address*: Bionanophotonic Systems Laboratory (BIOS, STI-IBI), Ecole Polytechnique Federale de Lausanne (EPFL), CH 1015 Lausanne, Switzerland

**Corresponding Author*:

M.-Carmen Estevez

NanoBiosensors and Bioanalytical Applications Group
Catalan Institute of Nanoscience and Nanotechnology (ICN2), CSIC and The Barcelona Institute of Science and Technology and CIBER-BBN
Campus de la UAB, Edifici ICN2
08193 Bellaterra (Barcelona) Spain

Tel:+34937374629

email:mcarmen.estevez@cin2.es

ABSTRACT

Colorectal cancer is treatable and curable when detected at early stages. However there is a lack of less invasive and more specific screening and diagnosis methods which would facilitate its prompt identification. Blood circulating autoantibodies which are immediately produced by the immune system at tumor appearance have become valuable biomarkers for preclinical diagnosis of cancer. In this work, we present the rapid and label-free detection of colorectal cancer autoantibodies directly in blood serum or plasma using a recently developed nanoplasmonic biosensor. Our nanoplasmonic device offers sensitive and real-time quantification of autoantibodies with excellent selectivity and reproducibility, achieving limits of detection around 1 nM (150-160 $ng \cdot mL^{-1}$). A preliminary evaluation of clinical samples of colorectal cancer patients has shown good correlation with ELISA. These results demonstrate the reliability of the nanobiosensor strategy and pave the way towards the achievement of a sensitive diagnostic tool for early detection of colorectal cancer.

Keywords

nanoplasmonic biosensor; plasma; serum; colorectal cancer; autoantibodies; clinical diagnosis

Abbreviations

CRC colorectal cancer

ELISA enzyme-linked immunosorbent assay

LSPR localized surface plasmon resonance

POC point of care

RI refractive index

SAM self-assembled monolayer

TAA tumor-associate antigen

1. Introduction

Colorectal cancer (CRC) is a worldwide health problem with an incidence over 1 million annual cases and being a major cause of morbidity and mortality in developed countries [1]. It is the third most common cancer and the fourth most common cause of death around the world. Despite the exact cause for CRC is not known, several risk factors have been established for the disease, including genetic and epigenetic parameters [2]. Familiar history of colon cancer or inflammatory diseases, age, lifestyle and environmental conditions are strongly associated to CRC development. CRC is easily curable when detected early [2], thereby prevention and regular screening play crucial roles in the fight against this cancer. However, CRC diagnosis is particularly challenging. The most reliable diagnosis technique is *via* sampling of colon biopsies suspected of possible tumor development, which is typically done during colonoscopy or sigmoidoscopy for the distal colon and rectum [3]. These procedures are highly invasive and present important limitations in terms of costs, available resources and low compliance. On the other hand, established noninvasive tests such as the guaiac-based fecal occult blood test (gFOBT) suffer from low specificity leading to inaccurate diagnosis results [4]. There is an evident need for novel screening tools, ideally, analytical techniques based on blood analysis, which permit the early and reliable identification and diagnosis of CRC. Development of blood biomarker assays that could indicate that a cancerous process is triggered would represent a great benefit. However, although a few serum proteins have been described as biomarkers in CRC (carcinoembryonic antigen (CEA), CA19.9 or CA125), none of them are recommended for early clinical diagnosis but for advanced stages and for monitoring recurrence of the disease [5].

Over the past decade, cancer research has made major advances in understanding the causes of developing CRC as well as the molecular mechanisms involved in the disease [6]. For instance many solid tumors such as breast, lung or colon cancer have revealed to be immunogenic. These tumors express aberrant levels of mutated or modified proteins known as tumor-associated antigens (TAA), which are related to the malignant growth. Such proteins can stimulate cellular and humoral immune response, triggering specific autoantibody production [7,8]. The role of autoantibodies in cancer is still unclear. It is not well-known whether they play a cancer-promoting role, an anti-tumor effect or if

they are an epiphenomenon associated to inflammation and tumor progression [9]. Nevertheless, autoantibody responses to TAAs hold promising characteristics to consider them as blood biomarkers for cancer detection and they are currently being investigated as potential diagnostic tools in multiple cancer types. Some reports have described the use of autoantibodies for early and preclinical detection of cancer, such as lung [10,11] or breast cancer [12]. The analysis of autoantibodies offers significant benefits when compared to direct determination of protein antigens associated to the tumor. Whereas detection of directly tumor-shed proteins in serum may be challenging due to their low abundance or to the difficulty of identifying simple mutations or structural modifications, serum autoantibodies are highly stable biomolecules and are produced in large quantities even after stimulation by a minimal amount of tumor antigen [12,13]. As a result, TAA-specific serum autoantibodies can constitute excellent circulating reporters for early and preclinical cancer diagnosis [14,15]. In the particular case of colorectal cancer, over 100 individual TAAs have been identified as target for autoantibody production, including full-length proteins, peptides, phage-peptides or glyco-peptides [14,16-18]. Current efforts in CRC research are directed not only to define specific TAA panels but also to develop efficient and highly sensitive analytical methods capable of detecting TAA autoantibodies in serum with optimum accuracy and reliability [19,20]. Most commonly employed methodologies are based on ELISA or protein microarrays [21] which are usually aimed at finding relative cut-off values, so far providing qualitative or semi-quantitative results. Optical biosensors can offer a valuable alternative in terms of time and sample consumption and can provide accurate quantification, which may result useful from a diagnosis point of view. Photonic and plasmonic biosensors in particular have shown great promise for the development of high-throughput and miniaturized platforms capable of carrying out label-free and highly sensitive biochemical analysis [22,23].

In this paper, we show the design and optimization of a nanoplasmonic-based biosensor for the direct detection and quantification of specific CRC-related TAA autoantibodies. We employ a refractometric nanoplasmonic biosensor whose configuration is based on the Localized Surface Plasmon Resonance (LSPR) of gold nanodisks [24]. The gold nanodisks are fabricated by hole-mask colloidal lithography [25] which is an easy, fast, low-cost and well-stablished methodology which

leads to reproducible results, with controlled density of disks on the surface. This device is highly sensitive to local refractive index (RI) changes occurring in close proximity to the surface of the transducer (in this case the gold nanodisks), such as the ones originated from biomolecular interactions. These RI changes can be detected as variations of the LSPR, which permits the real-time monitoring of the biorecognition events under label-free conditions. This nanoplasmonic biosensor has demonstrated excellent capabilities in terms of RI sensitivity improvement and signal-to-noise ratio enhancement, compared for instance with conventional Surface Plasmon Resonance [26] and more specifically its performance has also been validated for accurate detection of clinical biomarkers and antibodies in blood serum in few minutes[26,27]. The proposed biosensor strategy would allow rapid and simple analysis of TAA autoantibodies, providing a unique and innovative tool for CRC diagnosis.

2. Experimental

2.1. Materials

Main chemical reagents and salts for buffer preparation and biofunctionalization procedure were acquired from Sigma-Aldrich (Germany): alkanethiols for self-assembled monolayer (SAM) formation (16-mercaptohexadecanoic acid (MHDA) and 11-mercaptoundecanol (MUOH)), reagents for carboxylate group activation (1-ethyl-4(3-dimethylaminopropyl)carbodiimide hydrochloride (EDC) and N-hydroxysulfosuccinimide (s-NHS)), ethanolamine and Tween 20. Poly-L-Lysine-graft-PEG (MW~70000 $g \cdot mol^{-1}$ was purchased to SuSoS (Switzerland). Commercial serum was obtained from Sigma-Aldrich (Germany) and commercial plasma was purchased to Innovative Research (USA). cDNA encoding for full-length human genes EDIL3 and GTF2B in pDONR221 were obtained from the PlasmId repository (Harvard Institute of Proteomics) and, then, subcloned into pET28a (Novagen) for protein expression. TAAs were expressed in bacteria and purified according to previous studies [16,28]. The Institutional Ethical Review Boards of the Centro de Investigaciones Biológicas (CIB), the Spanish National Research Council (CSIC) and Hospital de Cabueñes (Gijón) approved this study on biomarker discovery in colorectal cancer. Serum samples were obtained from

the Hospital of Cabueñes previous informed consent of the patients. Antibodies anti-GTF2b and anti-EDIL3 were purchased to Santa Cruz Biotechnology (USA) and Abcam (UK), respectively.

2.2. Description of the Nanoplasmonic Biosensor

The nanoplasmonic device is based on a recently implemented LSPR sensing scheme based on a waveguided electromagnetic mode that arises in thin monolayers of sparse and randomly distributed plasmonic nanoparticles. Nanoplasmonic chips consist of short-range ordered arrays of gold nanodisks (diameter D = 100 nm, height H = 20 nm (Ti/Au 1/19 nm), surface density F = 6-7%) fabricated by hole-mask colloidal lithography (HCL) on glass substrates [25]. A detailed description of the fabrication process has been included in the Supplementary Material. Sensor chips are clamped between a trapezoidal glass prism (n=1.52) contacting the samples through RI matching oil (n≈1.512) and a custom-made Delrin flow cell (volume=4 μL). The flow cell is connected to a microfluidic system consisting on a syringe pump (New Era, NE-1000, USA) with adjustable pumping speed that ensures a constant liquid flow and a manually operated injection valve (IDEZ Health and Science, V-451, USA). For LSPR excitation, gold nanodisks are illuminated with a collimated halogen light (HL-2000, Micro-pack, USA) set in transverse-electric (TE) polarization mode at an angle of incidence of 80°. The reflected light is collected and fiber-coupled to a CCD spectrometer (Ocean Optics, Jazz Module, US). Reflectivity spectra are acquired every 3 ms, and 300 consecutive spectra are averaged to provide the spectrum to be analyzed. Excitation at 80° results in deep reflectivity dips at $\lambda_{LSPR} \approx$ 750 nm that lead to optimal biosensor performance [24,26]. Biomolecular interactions taking place close to the gold nanodisks induce RI changes on the surface and, as a consequence, wavelength displacements ($\Delta\lambda_{LSPR}$). Tracking of the real-time resonance peak position is achieved via polynomial fit using homemade readout software.

2.3. Surface functionalization

Prior to surface functionalization, sensor chips were subjected to a cleaning procedure consisting of consecutive 1 min sonication cycles in acetone, ethanol and MilliQ water, respectively, dried with N_2 stream and placed in a UV/O_3 generator (BioForce Nanoscience, USA) for 20 min, after which they

were rinsed with ethanol and water and dried with N_2. Formation of the alkanethiol SAM was carried out by coating the chip with 250 µM MHDA in ethanol for 5h at room temperature. Then, surface was rinsed with ethanol and water and dried with N_2 stream. For the activation of the carboxylic groups, the chip was incubated with 0.2 M EDC/0.05 M s-NHS in MES buffer (0.1 M pH 5.5) for 20 min at RT and then rinsed with water and dried. The surface was then immediately immersed in the TAA solution in PBS (10 mM pH 7.4) and incubated overnight at 4°C. Finally, biofunctionalized sensors were carefully rinsed with PBS and water, dried with N_2 stream and mounted in the platform. The non-sensing glass areas were subsequently coated with PLL-g-PEG (0.5 $mg \cdot mL^{-1}$) to avoid non-specific adsorptions. Figure S3 in Supplementary Material summarizes the biofunctionalization protocol.

2.4. Antibody detection assays

For antibody analysis, PBST 0.5% (PBS + 0.5% Tween 20) was settled as running buffer. Different concentrations of specific antibody were diluted in PBST 0.5% or in commercial serum/plasma and flowed over the functionalized surface at 25 $\mu L \cdot min^{-1}$ (See Figure S9 for an example of real time senrograms for the detection of specific antibodies at different concentrations). Regeneration of the surface was achieved by injecting 20 mM NaOH at 65 $\mu L \cdot min^{-1}$. Calibration curves were fitted to a saturation total binding model. Limit of detection (LoD) was calculated as the concentration corresponding to the blank signal plus three times its standard deviation (SD), while limit of quantification (LoQ) was determined as the concentration corresponding to the minimum measurable signal, set as the blank signal plus 10 times SD. Data analysis was performed using Origin Pro software. ELISA was carried out as previously described [16,28]. Briefly, microtiter plates (Maxisorp, Nunc) were coated overnight with 0.3 µg of the purified recombinant proteins, using GST and human Annexin IV as negative controls in 50 µl of PBS. After washing three times with PBS, plates were blocked with 3% skimmed milk in PBS (MPBS) for 2 h at room temperature. Then, serum samples (dilution, 1:100 in 3% MPBS) were incubated for 2 h at room temperature. After washing, peroxidase-labeled anti-human IgG (Jackson laboratories) (dilution, 1:500 in 3% MPBS) was added for 2 h at room temperature. Then, the signal was developed with 3,3´,5,5´-tetramethylbenzidine

substrate for 10 min (Sigma-Aldrich). The reaction was stopped with 1 M HCl, and absorption measured at 450 nm.

3. Results

3.1. Description of the Nanoplasmonic Biosensor Platform

The nanoplasmonic device is based on a recently implemented LSPR sensing scheme based on a waveguided electromagnetic mode that arises in thin monolayers of sparse and randomly distributed plasmonic nanoparticles [24]. We previously reported that the in-plane LSPR excitation strongly enhances the polarizability of the nanodisks, creating an effective RI that is sufficiently large to support a guided electromagnetic mode inside the plasmonic monolayer. Both the nanoparticle surface density (F) and the incidence angle of light are key aspects that affect this sensing performance. Surface density was precisely chosen so that the optimal mode excitation (light coupling efficiency close to 100%) occurs at angles where the sensitivity was maximized (angle close to 90º). In particular we employ short-ordered arrays of gold nanodisks (diameter D = 100 nm, height H = 20 nm, surface density F = 6-7%) fabricated by hole-mask colloidal lithography (HCL) (See experimental details in Supplementary Material). This nanofabrication technique allows simple, cost-efficient and wafer-scale production of the nanoplasmonic chips. This waveguided mode results not only in a large increase of the RI sensitivity, but also strongly improves the signal-to-noise ratio. Both effects assure an overall improved RI sensing performance that is up to one order of magnitude better than that of isolated non-interacting nanodisks. Thus, RI changes occurring close to the nanodisk surfaces are much easier to detect. A schematic representation of the biosensor can be seen in Figure 1a. For LSPR excitation, the nanoplasmonic chip is illuminated with a broadband polarized light at a determined angle of incidence (Θ = 80°) [24,26], and the reflected light is collected with a spectrophotometer. The obtained spectra show a deep reflectivity dip at $\lambda_{LSPR} \approx 750$. Biomolecular interactions occurring on the nanodisks surfaces generate RI changes that, in turn, cause displacements of the spectral LSPR peak ($\Delta\lambda_{LSPR}$) (red shifts when binding occurs and blue shifts during a desorption process). The real-time interrogation of this $\Delta\lambda_{LSPR}$ enables the extraction of

quantitative information related to the biomolecular interactions taking place in a label-free manner (Figure 1.B). In addition, the designed optical platform has very small dimensions (all optical components are mounted on a 20 x 20 cm^2 portable breadboard), exemplifying its facile miniaturization and potential portability.

3.2. Design and Optimization of the Sensor Biofunctionalization

Among the numerous TAAs defined for colorectal cancer [18], we selected GTF2b (general transcription factor IIB) and EDIL3 (EGF-like repeats and discoidin I-like domain 3 protein) since both proteins have been previously evaluated as possible TAA targets for autoantibody production in colorectal cancer [14]. A study performed in cancer-induced animals provided evidences of immediate production of GTF2b and EDIL3 autoantibodies, among others [14]. The presence of autoantibodies was detectable at a very early stage in tumor development, even before adenoma formation. Especially, GTF2b could be detected before clinically observable symptomatology while EDIL3 is characterized by a more homogeneous but late response. This makes GTF2B more appropriate to enhance sensitivity while EDIL3 would enhance specificity.

In order to directly detect the autoantibodies for these two TAA, a biosensing strategy based on the direct immobilization of the TAA on the surface of the gold nanodisks has been addressed. A schematic representation of the proposed biosensor strategy is showed in Figure 1C. Biofunctionalization of the nanoplasmonic sensor chip was based on the formation of a functional alkanethiol self-assembled monolayer (SAM) specifically onto the gold nanodisks *via* thiol chemisorption, which act as linker for the covalent attachment of the antigens. We employed 16-mercaptohexadecanoic acid (MHDA) to create a tight and uniform SAM where the carboxylic groups of the MHDA are activated to readily react with lysine (Lys) residues available in the proteins. The reaction generates an amide bond between the protein and the SAM. The grafting density of antigen molecules on the surface can also be controlled by introducing a lateral spacer during the formation of the SAM (i.e. 11-mercaptoundecanol, MUOH). In parallel, glass substrate was coated with the copolymer poly-L-lysine PEG (PLL-g-PEG 0.5 $mg \cdot mL^{-1}$) to prevent and minimize possible undesired

adsorptions. The PLL-g-PEG coating generates a highly hydrophilic layer that has demonstrated to effectively reduce nonspecific binding of proteins and other compounds present in biological matrices. This step facilitates the direct measurement in these biological fluids when using label-free biosensors [26,29].

To establish the best immobilization conditions for both TAAs, the nanoplasmonic chips were independently biofunctionalized with recombinant human GTF2b and EDIL3 proteins employing different molar ratios of mixed alkanethiol SAM (MHDA/MUOH 1:0, 1:1, 1:10) at a total thiol concentration of 250 μM. The immobilization procedure was carried out *in situ* over the SAM-functionalized chip already mounted on the sensor platform, by flowing the protein solution and monitoring the covalent coupling process (Figure S4 in Supplementary Material). We compared the immobilization signals obtained with a fixed protein concentration (50 $\mu g \cdot mL^{-1}$) over the different SAM ratios. We selected 50 $\mu g \cdot mL^{-1}$ based on preliminary experiments performed with a conventional SPR biosensor. We observed that although higher concentrations of protein (i.e. 100 $\mu g \cdot mL^{-1}$) rendered higher immobilization signal, the subsequent detection of the autoantibody (at a fixed concentration of 1 $\mu g \cdot mL^{-1}$) remained similar to the one obtained with a protein concentration of 50 $\mu g \cdot mL^{-1}$ (see Figure S5 in the Supplementary Material). This was indicative of a more optimum coverage of the surface for detection purposes with 50 $\mu g \cdot mL^{-1}$ than with 100 $\mu g \cdot mL^{-1}$. Based on these results and on previous conditions optimized for protein attachment to SAMs [27] we selected 50 $\mu g \cdot mL^{-1}$ of protein for further experiments. The highest amount of protein was attached to the sensor surface when maximum carboxylic density was employed (Figure S6a in Supplementary Material), inducing wavelength shifts around 3 nm. This was observed for both GTF2b and EDIL proteins. Introduction of spacer molecules (MUOH) to the SAM resulted in lower signals thereby indicating less amount of TAA immobilized. However, the optimum TAA layer, which will lead to better detection levels, does not necessarily require maximum coverage with proteins. The appropriate distribution of antigens on the surface reveals itself as an important factor to favor the accessibility of antibodies. Control of the spacing between TAA molecules can *a priori* modulate possible steric hindrance effects and improve the ability of the antibodies to interact. We evaluated the detection

efficiency by flowing a 1 $\mu g \cdot mL^{-1}$ specific antibody solution over the corresponding GTF2b and EDIL3 functionalized surfaces. This concentration was selected for screening purposes in order to choose the best immobilization conditions before performing a full calibration curve. In addition, TAA immobilization procedure was also carried out *ex situ*, by coating the functionalized sensor chip with the protein overnight, rinsing it with buffer and then installing the protein-modified chip in the biosensor. The antibody detection signal achieved for both *ex situ* and *in situ* procedures carried out with mixed alkanethiol SAMs at different molar ratios was compared and is summarized in the Figure S6b in the Supplementary Material). No steric hindrance effects appeared to be relevant for the concentration of TAA tested (50 $\mu g \cdot mL^{-1}$) as maximum antibody detection was obtained in all cases when maximum carboxylic density was used (MHDA/MUOH 1:0). This suggests that the immobilization of TAAs at the selected concentration on alkanethiol SAMs formed exclusively with MHDA actually provides highly efficient bioreceptor layers, as also previously reported [30]. It can also be appreciated that *ex situ* immobilization resulted in significant higher antibody signals for the same concentration of immunoreagents. This could be attributed to a more efficient coupling yield and also to a more efficient protein rearrangement on the surface facilitated by longer reaction times (protein coupling overnight *vs.* 30 min when it is done *in situ*). From the above results, overnight immobilization of TAA over a 100% MHDA SAM was selected as optimum biofunctionalization strategy for further experiments. Regeneration for a potential reutilization of the TAAs functionalized surfaces was also evaluated. For both TAA-modified surfaces – GTF2b and EDIL3 – basic conditions (20 mM NaOH) disrupted the TAA-antibody interaction without altering or modifying the immobilized proteins (Figure S7 and S8 in Supplementary Material). Under these conditions it was possible to reuse the functionalized surface with good repeatability for up to 100 cycles before progressive decrease of the antibody detection signals.

Calibration curves for both anti-GTF2b and anti-EDIL3 (Figure 2A and 2B) were then performed in standard buffer conditions (i.e. PBS with 0.5% of Tween 20 (PBST)), which according to previous works helped drastically reduce nonspecific adsorptions onto the sensor chip) [26,27]. Different antibody concentrations ranging from 50 $ng \cdot mL^{-1}$ to 1 $\mu g \cdot mL^{-1}$ were flowed by triplicate through the

specific TAA functionalized surfaces, respectively, and the resonance shift was obtained (Figure 2A and 2B). Limits of detection (LoD) were determined as the minimum antibody concentrations that provide an observable signal (i.e. blank signal plus 3 times its standard deviation). The LoD for anti-GTF2b assay was 10 $ng \cdot mL^{-1}$ (66 pM) and 5 $ng \cdot mL^{-1}$ (33 pM) for anti-EDIL3 assay. Limits of quantification (LoQ) were determined as the minimum measurable signal, being 34 $ng \cdot mL^{-1}$ (227 nM) and 19 $ng \cdot mL^{-1}$ (127 pM) for GTF2b and EDIL3, respectively. Besides, the specificity of the assays was confirmed by using nonspecific antibodies as control. Measurements of anti-GTF2b over an EDIL3-functionalized surface and *vice versa* led to negligible signals (Figure 2A and 2B, red lines), which corroborates the signal contribution solely comes from the specific antibody recognition and confirms the feasibility of the methodology for antibody quantification. Excellent reproducibility and stability of the biosensor-based assays were finally demonstrated by performing intra- and inter-assays (curves performed in the same nanodisk-functionalized surface and in different surfaces, respectively). As it can be seen in Table 1, the coefficient of variation (CV) for both GTF2b and EDIL3 was below the maximum variability recommended for clinical analysis (~15%) [31], both for the LoD and for the maximum signal (S_{max}), taken at the maximum antibody concentration tested ([Ab] = 1 $\mu g \cdot mL^{-1}$).

3.3. Analysis of TAA Antibodies in Serum and Plasma

In order to evaluate the influence of the matrix, commercial serum (undiluted, and diluted 1:1 and 1:10 in PBST) and commercial plasma (undiluted, and diluted 1:1 and 1:10 in PBST) were flowed over the biofunctionalized nanoplasmonic surfaces (i.e. TAA layer + PLL-g-PEG coating) (Figure 3). As it can be seen in the sensorgrams, in both cases a significant background signal was observed due to the binding of fluid components onto the bioactive layer, being slightly higher for undiluted plasma (whose difference compared to serum is the presence of fibrinogen). A 1:10 dilution in PBST was necessary to achieve a complete reduction of nonspecific adsorptions for both fluids, resulting in virtually no background signals.

Besides the influence of the nonspecific binding onto the surface, possible matrix effects on the interaction of the antibody with the TAA-coated layer can occur, altering the analysis features. In order to assess this undesired effect, both GTF2b and EDIL3 calibration curves were obtained by spiking serum or plasma with several known concentrations of antibodies and then diluting them in PBST (1:10) (Figure 4). The curves were analogous to those obtained with standard buffer conditions although a slight increase of the LoDs was observed. This minor worsening can be attributed to a possible hindrance of the antibody/TAA interaction. For the GTF2b antibody, the LoD was 16 $ng \cdot mL^{-1}$ in diluted serum and 15 $ng \cdot mL^{-1}$ in diluted plasma, compared to a LoD of 10 $ng \cdot mL^{-1}$ in buffer. In the case of EDIL3 antibody detection, LoDs were 12 $ng \cdot mL^{-1}$ in diluted serum and 11 $ng \cdot mL^{-1}$ in diluted plasma, compared to 5 $ng \cdot mL^{-1}$ in buffer. Overall the sample dilution (1:10) has inevitably decreased the sensitivity over one order of magnitude, with detectabilities around 150-160 $ng \cdot mL^{-1}$ for GTF2b and around 110-120 $ng \cdot mL^{-1}$ for EDIL3, respectively depending on the fluid.

Clinical serum samples from CRC patients were analyzed with the nanoplasmonic biosensor for a preliminary assessment of the viability of our approach. Serum samples collected from patients from the Hospital of Cabueñes (Gijón, Spain) with diagnosed CRC and samples from healthy individuals were evaluated employing the optimal conditions selected before (1:10 dilution with PBST). All samples were previously analyzed for the presence of GTF2b autoantibodies using semi-quantitative ELISA, so the absolute concentration of the target biomarker was unknown. Table 2 compares the concentration values obtained with the nanoplasmonic biosensor (in $\mu g \cdot mL^{-1}$) to absorbance values (in optical density units, OD) obtained with the ELISA (quantitative data is not commonly determined with the ELISA for autoantibodies). A consistent correlation was observed in terms of relative signals. Negative samples from healthy subjects resulted below the LoD established for our biosensor technique (160 $ng \cdot mL^{-1}$) while positive samples lead to relatively high signals (i.e. high concentration of GTF2b autoantibodies).

4. Discussion

A major challenge in colorectal cancer research focuses on the development of novel diagnostic techniques for simple, rapid and accurate detection of the disease at earlier stages. In this regard,

cancer-associated autoantibodies generated by the immune system during tumor appearance have evidenced its high value as blood-circulating biomarkers for preclinical cancer diagnosis. We propose the use of an innovative nanoplasmonic biosensor for the direct and label-free quantification of CRC autoantibodies in serum or plasma. Our nanoplasmonic biosensor offer real-time detection of TAA antibodies without the need of any labels or sample pretreatments, which simplifies the analysis and provides interesting alternatives to develop small, fast and user-friendly point-of-care (POC) devices that could be used directly at doctor's office. The implementation of POC biosensors for rapid and reliable CRC screening could substantially afford a breakthrough towards non-invasive and highly specific diagnostic tools for this disease which in turn would help to improve patient survival rates.

The overall performance of the biosensor assay has been demonstrated for the determination of autoantibodies against two important CRC antigens: GTF2b and EDIL3. Both autoantibodies were selected as representative for the disease as they are generated at very early stages of CRC development and can be detected in blood serum before the onset of tumor lesions [14]. Biofunctionalization of the nanoplasmonic sensors has been designed to create a highly stable TAA layer that ensures an efficient capture of the specific antibodies. The immobilization strategy is based on the material-selective functionalization of the gold nanodisks through the formation of an alkanethiol SAM, which guarantees the biomolecular interaction to take place solely on the sensor spots. The PLL-g-PEG coating of the glass areas (which represents over the 94% of the surface) prevents the nonspecific binding to substrate. The covalent coupling of the TAA *via* the terminal amine groups of Lys residues is a simple and robust procedure that can be applied to immobilize virtually all proteins. Several biofunctionalization conditions have been optimized (e.g. alkanethiol SAM ratios, binding time, etc.) for the enhancement of the antibody capture efficacy reaching a LoD of 10 $ng \cdot mL^{-1}$ (~ 66 pM) for GTF2b antibody and 5 $ng \cdot mL^{-1}$ (~ 33 pM) for EDIL3 antibody in standard buffer, showing in both cases high selectivity and reproducibility. A complete assay cycle (including regeneration) is accomplished in 30 min. Besides, the bioactive surface with the immobilized TAA has proven to be reusable for more than 100 cycles with good repeatability.

An ultimate goal in POC development relies on the ability to readily detect the biomarkers in biological fluids. Here, we have exploited the unique hydrophilic properties of the PLL-g-PEG coating layer together with the use of a dilution buffer containing a high concentration of surfactant (Tween 20) in order to minimize possible interferences coming from serum or plasma matrices. In particular, a simple dilution of the biological sample 1:10 with PBST has led to a complete removal of background signals enabling the direct quantification without requiring purification or other extra pretreatments. This dilution factor inevitably increases the limit of detection. However, it is much lower than the minimum dilution required in the ELISA assay. Overall the features of the resultant calibration curves, both in diluted serum and plasma, offer a highly reliable analysis method to quantify the TAA autoantibodies with elevated selectivity and reproducibility. Moreover, clinical samples analysis further demonstrates the potential of using this device in comparison to conventional ELISA methods, according to the good correlation observed for the detection of GTF2b antibodies in CRC-diagnosed patients and healthy individuals. In this regard, a more complete quantitative clinical validation will be required in the future. However, to our knowledge, serological concentration levels of CRC autoantibodies have not been fully established so far, as most research articles in the field especially focus on their identification and the assessment of their diagnostic and/or prognostic value. Nevertheless we cannot obviate the evident usefulness of knowing this concentration value compared with other semi-quantitative or qualitative methods, not only from a perspective of early diagnosis but also for disease follow-up. Besides, the possibility of quantifying autoantibodies concentration in serum samples may allow further comprehension of the humoral response triggered by the tumor and harness the basis for the improvement of prognosis of the disease. On-going work currently focuses on the improvement of biofunctionalization strategies and the use of antifouling agents that permit direct measurements of undiluted serum and plasma, therefore enhancing the detectability at least 10-fold. Moreover, the biofunctionalization methodology developed can be easily adjusted for any TAA with potential interest. This facilitates the eventual expansion of the biosensor strategy to elaborate a multiplexed compact analytical platform for the simultaneous detection of a CRC-specific panel of autoantibodies, which is ultimately necessary to fully cover the patient variability and to maximize the sensitivity and specificity of the method.

5. Conclusions

We have developed a novel analytical label-free strategy for the detection of tumor-associated autoantibodies in blood serum and plasma based on an innovative nanoplasmonic biosensor technology. This strategy could provide a reliable and non-invasive screening and diagnosis of colorectal cancer at early stages. Our biosensor allows the label-free quantification of specific CRC-related autoantibodies in few minutes, without requiring any sample purification or pretreatment. Several biofunctionalization parameters have been optimized, reaching a limit of detection of 1 nM (150-160 $ng \cdot mL^{-1}$) for direct measurements in human serum or plasma. Selectivity and reproducibility of the assay have been also evaluated demonstrating the excellent accuracy and robustness of the biosensor. The analysis of clinical samples from colorectal cancer patients has shown good correlation with ELISA. Overall, the results obtained highlight the exceptional potential of our nanoplasmonic biosensor as a tool for the early detection of colorectal cancer and current efforts are focused on establishing a multiplexed approach to expand the strategy to a CRC-panel of autoantibodies.

Acknowledgements

M. Soler acknowledges financial support from "Programa de Formación de Personal Investigador (FPI)" from the Spanish Ministry of Economy and Competitiveness (MINECO). R. Villar-Vazquez was a recipient of a FPU fellowship from the Spanish Ministry of Education and Culture. We acknowledge the financial support from COLONTEST project (RETOS-COLABORACIÓN Subprogram, RTC-2014-1518-1). The NanoB2A is a consolidated research group (Grup de Recerca) of the Generalitat de Catalunya and has support from the Departament d'Universitats, Recerca i Societat de la Informació de la Generalitat de Catalunya (2014 SGR 624). ICN2 is the recipient of Grant SEV-2013-0295 from the "Severo Ochoa Centers of Excellence" Program of Spanish MINECO. In addition, JI Casal was supported by the grant BIO2012-31023 from the MINECO.

References

[1] A. Jemal, F. Bray, M.M. Center, J. Ferlay, E. Ward, D. Forman, Global cancer statistics, CA Cancer J. Clin. 61 (2011) 69-90.

[2] F.A. Haggar, R.P. Boushey, Colorectal cancer epidemiology: incidence, mortality, survival, and risk factors, Clin. Colon Rectal Surg. 22 (2009) 191.

[3] S. Winawer, R. Fletcher, D. Rex, J. Bond, R. Burt, J. Ferrucci, T. Ganiats, T. Levin, S. Woolf, D. Johnson, Colorectal cancer screening and surveillance: clinical guidelines and rationale—update based on new evidence, Gastroenterology 124 (2003) 544-560.

[4] B.-A. Adelstein, P. Macaskill, S.F. Chan, P.H. Katelaris, L. Irwig, Most bowel cancer symptoms do not indicate colorectal cancer and polyps: a systematic review, BMC Gastroenterol. 11 (2011) 65-65.

[5] M. Duffy, A. Van Dalen, C. Haglund, L. Hansson, E. Holinski-Feder, R. Klapdor, R. Lamerz, P. Peltomaki, C. Sturgeon, O. Topolcan, Tumour markers in colorectal cancer: European Group on Tumour Markers (EGTM) guidelines for clinical use, Eur. J. Cancer 43 (2007) 1348-1360.

[6] N. The Cancer Genome Atlas, Comprehensive Molecular Characterization of Human Colon and Rectal Cancer, Nature 487 (2012) 330-337.

[7] C.A. Casiano, M. Mediavilla-Varela, E.M. Tan, Tumor-associated antigen arrays for the serological diagnosis of cancer, Mol. Cell. Proteomics 5 (2006) 1745-1759.

[8] W. Liu, B. Peng, Y. Lu, W. Xu, W. Qian, J.-Y. Zhang, Autoantibodies to tumor-associated antigens as biomarkers in cancer immunodiagnosis, Autoimmun Rev 10 (2011) 331-335.

[9] S. Kobold, T. Lütkens, Y. Cao, C. Bokemeyer, D. Atanackovic, Autoantibodies against tumor-related antigens: incidence and biologic significance, Hum. Immunol. 71 (2010) 643-651.

[10] P. Boyle, C. Chapman, S. Holdenrieder, A. Murray, C. Robertson, W. Wood, P. Maddison, G. Healey, G. Fairley, A. Barnes, Clinical validation of an autoantibody test for lung cancer, Ann. Oncol. 22 (2011) 383-389.

[11] J. Qiu, G. Choi, L. Li, H. Wang, S.J. Pitteri, S.R. Pereira-Faca, A.L. Krasnoselsky, T.W. Randolph, G.S. Omenn, C. Edelstein, Occurrence of autoantibodies to annexin I, 14-3-3 theta and LAMR1 in prediagnostic lung cancer sera, J. Clin. Oncol. 26 (2008) 5060-5066.

[12] C. Chapman, A. Murray, J. Chakrabarti, A. Thorpe, C. Woolston, U. Sahin, A. Barnes, J. Robertson, Autoantibodies in breast cancer: their use as an aid to early diagnosis, Ann. Oncol. (2007).

[13] Y. Hosono, M. Goto, D. Kobayashi, K. Kuribayashi, M. Tanaka, N. Watanabe, Diagnostic relevance of autoantibody detection against inhibitors of apoptosis proteins in colon cancer and colon adenoma, Mol. Clin. Oncol. 3 (2015) 595-600.

[14] R. Barderas, R. Villar-Vazquez, M.J. Fernandez-Acenero, I. Babel, A. Pelaez-Garcia, S. Torres, J.I. Casal, Sporadic colon cancer murine models demonstrate the value of autoantibody detection for preclinical cancer diagnosis, Sci. Rep. 3 (2013) 2938.

[15] Y.S. Cho-Chung, Autoantibody biomarkers in the detection of cancer, BBA-Mol Basis Dis 1762 (2006) 587-591.

[16] I. Babel, R. Barderas, R. Diaz-Uriarte, V. Moreno, A. Suarez, M.J. Fernandez-Acenero, R. Salazar, G. Capella, J.I. Casal, Identification of MST1/STK4 and SULF1 proteins as autoantibody targets for the diagnosis of colorectal cancer by using phage microarrays, Mol. Cell. Proteomics 10 (2011) M110 001784.

[17] R. Barderas, I. Babel, R. Diaz-Uriarte, V. Moreno, A. Suarez, F. Bonilla, R. Villar-Vazquez, G. Capella, J.I. Casal, An optimized predictor panel for colorectal cancer diagnosis based on the combination of tumor-associated antigens obtained from protein and phage microarrays, J. Proteomics 75 (2012) 4647-55.

[18] H. Chen, S. Werner, S. Tao, I. Zörnig, H. Brenner, Blood autoantibodies against tumor-associated antigens as biomarkers in early detection of colorectal cancer, Cancer Lett. 346 (2014) 178-187.

[19] F.J. Lowe, W. Shen, J. Zu, J. Li, H. Wang, X. Zhang, L. Zhong, A novel autoantibody test for the detection of pre-neoplastic lung lesions, Mol. Cancer 13 (2014) 78.

[20] M. Reuschenbach, J. Dörre, T. Waterboer, J. Kopitz, M. Schneider, N. Hoogerbrugge, E. Jäger, M. Kloor, M. von Knebel Doeberitz, A multiplex method for the detection of serum antibodies against in silico-predicted tumor antigens, Cancer Immunol Immun 63 (2014) 1251-1259.
[21] P. Zaenker, M.R. Ziman, Serologic Autoantibodies as Diagnostic Cancer Biomarkers—A Review, Cancer Epidemiol. Biomarkers Prev. 22 (2013) 2161-2181.
[22] M.C. Estevez, M. Alvarez, L.M. Lechuga, Integrated optical devices for lab-on-a-chip biosensing applications, Laser Photon Rev 6 (2012) 463-487.
[23] O. Tokel, F. Inci, U. Demirci, Advances in plasmonic technologies for point of care applications, Chem. Rev. 114 (2014) 5728-5752.
[24] M.A. Otte, M.C. Estévez, D. Regatos, L.M. Lechuga, B. Sepúlveda, Guiding Light in Monolayers of Sparse and Random Plasmonic Meta-atoms, ACS Nano 5 (2011) 9179-9186.
[25] H. Fredriksson, Y. Alaverdyan, A. Dmitriev, C. Langhammer, D.S. Sutherland, M. Zäch, B. Kasemo, Hole–Mask Colloidal Lithography, Adv. Mater. 19 (2007) 4297-4302.
[26] M. Soler, et al., Highly sensitive dendrimer-based nanoplasmonic biosensor for drug allergy diagnosis, Biosens. Bioelectron. 66 (2015) 115-123.
[27] M. Soler, M.-C. Estevez, M. Alvarez, M.A. Otte, B. Sepulveda, L.M. Lechuga, Direct detection of protein biomarkers in human fluids using site-specific antibody immobilization strategies, Sensors 14 (2014) 2239-2258.
[28] I. Babel, R. Barderas, R. Díaz-Uriarte, J.L. Martínez-Torrecuadrada, M. Sánchez-Carbayo, J.I. Casal, Identification of Tumor-associated Autoantigens for the Diagnosis of Colorectal Cancer in Serum Using High Density Protein Microarrays, Mol. Cell. Proteomics 8 (2009) 2382-2395.
[29] R. Marie, A. Dahlin, J. Tegenfeldt, F. Höök, Generic surface modification strategy for sensing applications based on Au/SiO2 nanostructures, Biointerphases 2 (2007) 49-55.
[30] J.-F. Masson, T.M. Battaglia, J. Cramer, S. Beaudoin, M. Sierks, K.S. Booksh, Reduction of nonspecific protein binding on surface plasmon resonance biosensors, Anal. Bioanal. Chem. 386 (2006) 1951-1959.
[31] A. Buick, M. Doig, S. Jeal, G. Land, R. McDowall, Method validation in the bioanalytical laboratory, J. Pharm. Biomed. Anal. 8 (1990) 629-637.

Figure Captions:

Figure 1. (a) Schematic representation of the miniaturized nanoplasmonic biosensor. A picture of the nanodisks and a SEM image of the actual shape of the gold nandisks fabricated on the glass substrate are also shown. **(b)** Graphs showing the resonance peak (photon counts *vs.* λ) *(left)* and the shift of the resonance peak over time ($\Delta\lambda_{LSPR}$ *vs.* time) *(right)*; **(c)** TAA biofunctionalization methodology based on covalent coupling to an alkanethiol SAM and subsequent antibody detection.

Figure 2. (a) Calibration curve for anti-GTF2b detection performed over GTF2b-biofunctionalized nanodisks (black). Red dashed line indicates nonspecific adsorption of a control antibody (anti-EDIL3); **(b)** Calibration curve for anti-EDIL3 detection performed over EDIL3-biofunctionalized nanodisks (black). Red dashed line indicates nonspecific adsorption of a control antibody (anti-GTF2b).

Figure 3. (a) Background signal corresponding to nonspecific adsorption of undiluted serum (black), serum diluted 1:1 in PBST 0.5% (purple) and serum diluted 1:10 in PBST 0.5% (green); **(b)** Background signal corresponding to nonspecific adsorption of undiluted plasma (blue), plasma diluted 1:1 in PBST 0.5% (orange) and plasma diluted 1:10 in PBST 0.5% (pink).

Figure 4. (a) Calibration curves for anti-GTF2b antibody detection in PBST buffer (black), serum diluted 1:10 in PBST (green) and plasma diluted 1:10 in PBST (pink); **(b)** Calibration curves for anti-EDIL3 antibody detection in PBST buffer (black), serum diluted 1:10 in PBST (green) and plasma diluted 1:10 in PBST (pink).

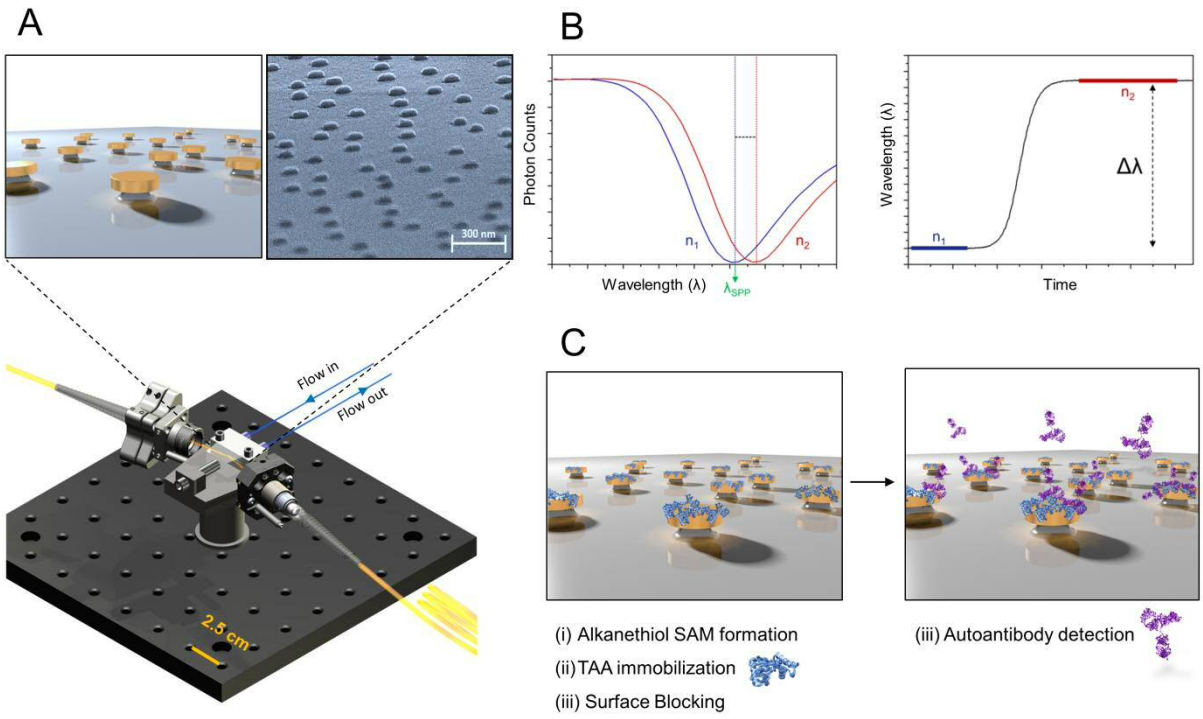
A
300 nm
Flow in
Flow out
2.5 cm
B
Photon Counts
Wavelength (λ)
λ_{SPP}
n_1
n_2
Wavelength (λ)
Time
n_1
n_2
Δλ
C
(i) Alkanethiol SAM formation
(ii) TAA immobilization
(iii) Surface Blocking
(iii) Autoantibody detection

Figure 1

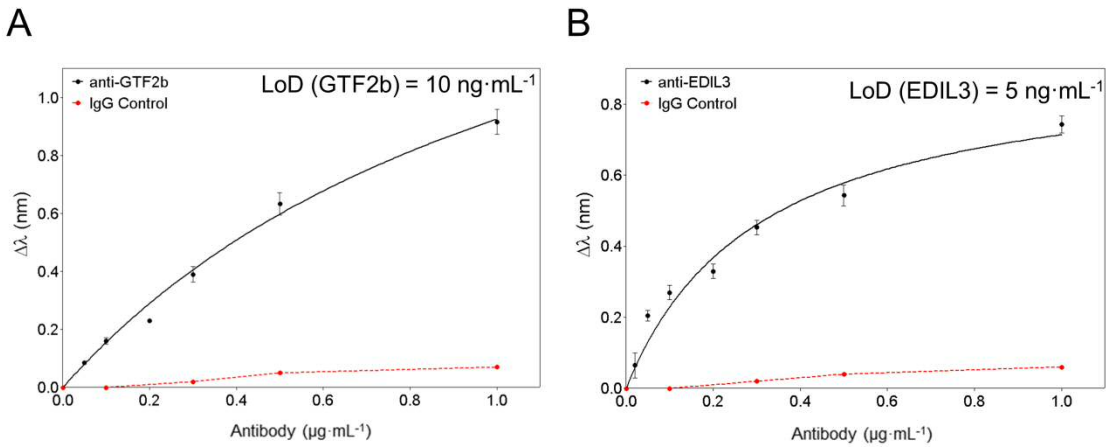
A
anti-GTF2b
IgG Control
LoD (GTF2b) = 10 ng·mL-1
Δλ (nm)
Antibody (µg·mL-1)
B
anti-EDIL3
IgG Control
LoD (EDIL3) = 5 ng·mL-1
Δλ (nm)
Antibody (µg·mL-1)

Figure 2

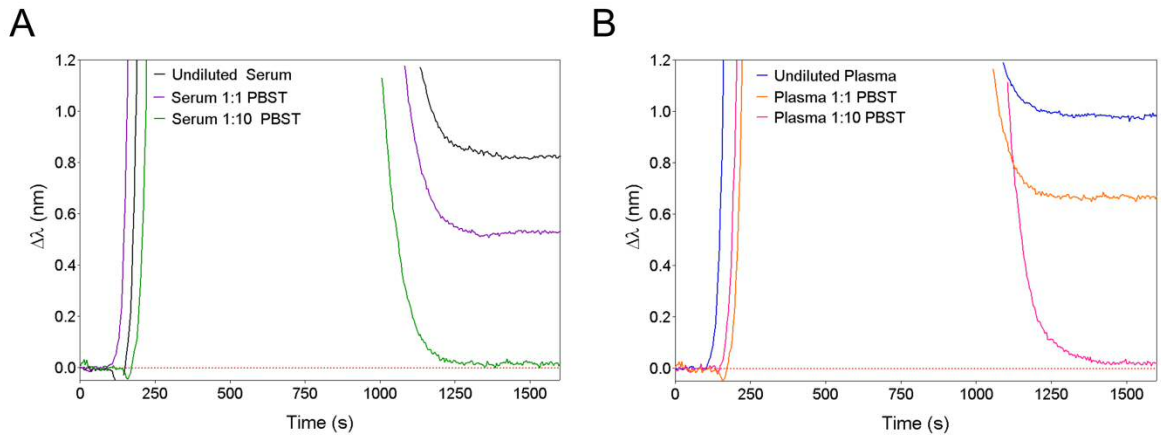
A
Undiluted Serum
Serum 1:1 PBST
Serum 1:10 PBST
Δλ (nm)
Time (s)
B
Undiluted Plasma
Plasma 1:1 PBST
Plasma 1:10 PBST
Δλ (nm)
Time (s)

Figure 3

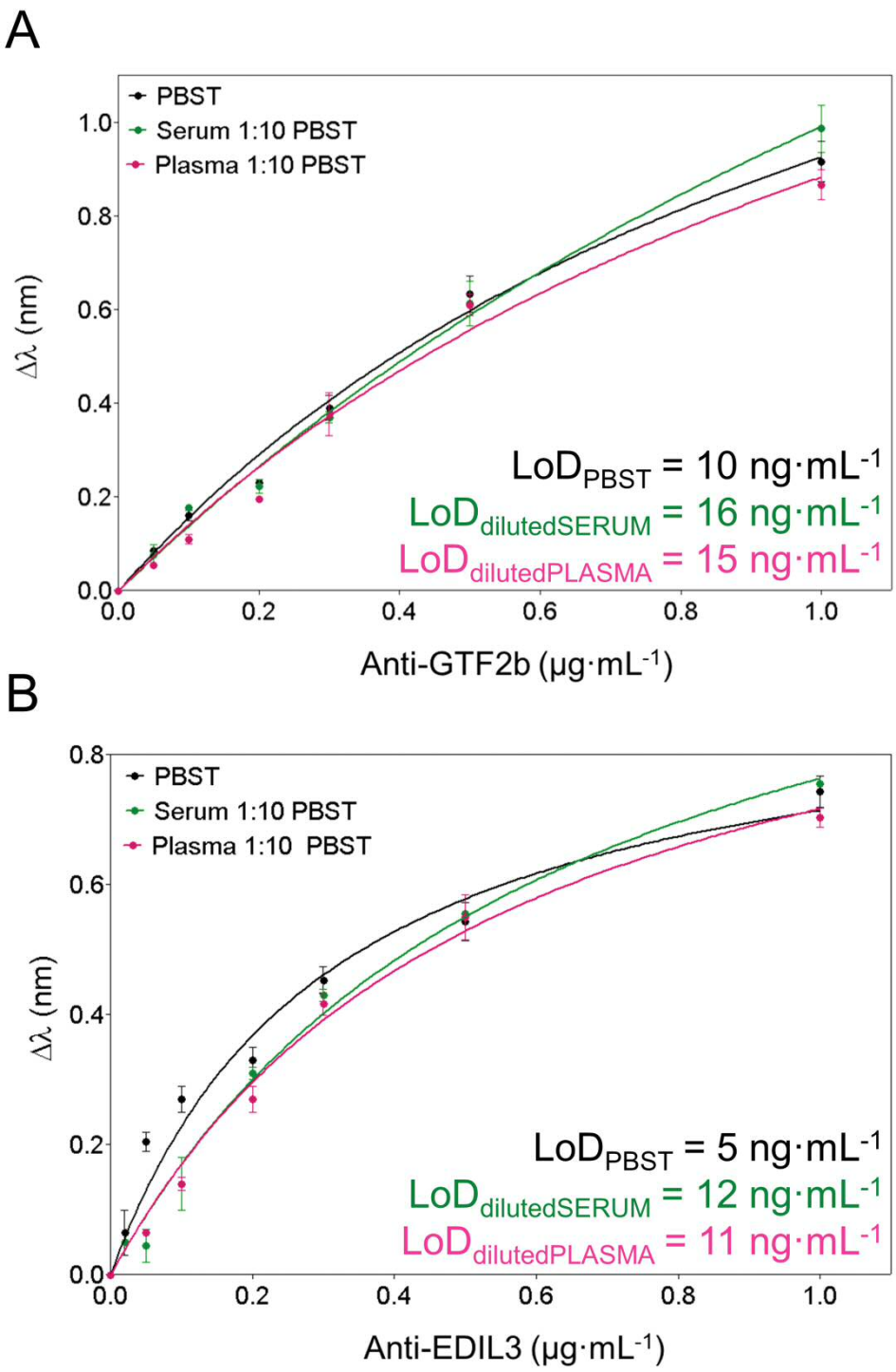
A
PBST
Serum 1:10 PBST
Plasma 1:10 PBST
Δλ (nm)
Anti-GTF2b (µg·mL-1)
LoDPBST = 10 ng·mL-1
LoDdilutedSERUM = 16 ng·mL-1
LoDdilutedPLASMA = 15 ng·mL-1
B
PBST
Serum 1:10 PBST
Plasma 1:10 PBST
Δλ (nm)
Anti-EDIL3 (µg·mL-1)
LoDPBST = 5 ng·mL-1
LoDdilutedSERUM = 12 ng·mL-1
LoDdilutedPLASMA = 11 ng·mL-1

Figure 4

Table 1. Inter and intra-assay features for GTF2b and EDIL3 antibodies detection with the nanoplasmonic biosensor

		GTF2b antibody		EDIL3 antibody	
		Mean ± SD*	**% CV**	**Mean ± SD**	**% CV**
Intra-assay	**LOD ($ng \cdot mL^{-1}$)**	9.7 ± 0.5	5.15	5.2 ± 0.2	3.77
	S_{max} (nm)	0.937 ± 0.0015	1.63	0.733 ± 0.016	2.08
Inter-assay	**LOD ($ng \cdot mL^{-1}$)**	10.1 ± 1.2	11.9	4.9 ± 0.4	8.16
	S_{max} (nm)	0.917 ± 0.07	8.19	0.743 ± 0.04	5.60

* Mean and standard deviation of 3 replicates

Table 2. Clinical serum samples analysis determined by ELISA and by the nanoplasmonic biosensor.

Sample		GTF2b Analysis Results	
		ELISA (OD)	**Nanobiosensor ($ng \cdot mL^{-1}$)***
G30	Negative	0.18	ND †
G42	Positive	0.48	175 ± 8
G56	Positive	0.56	254 ± 10
G101	Negative	0.13	ND †

***** Mean ± SD for 3 replicates

† ND: No Detected (below limit of detection: 160 $ng \cdot mL^{-1}$)